INTEGRATED GEOPHYSICAL INVESTIGATIONS AT GEMETO THERMAL SPRINGS, AWASSA, MAIN ETHIOPIAN RIFT

By

YIGREM ASSEFA DINGO

A thesis Submitted to the School of Graduate Studies of Addis Ababa University in partial fulfillment of the requirements for the Degree of Masters of Science in Exploration Geophysics

March 2007

ADDIS ABABA UNIVERSITY

DEPARTMENT OF EARTH SCIENCES

SCHOOL OF GRADUATE STUDIES

INTEGRATED GEOPHYSICAL INVESTIGATIONS AT GEMETO THERMAL SPRINGS, AWASSA, MAIN ETHIOPIAN RIFT

By

Yigrem Assefa Dingo

Faculty of Science

Department of Earth Sciences

Approved by board of examiners:

Dr. Balemawal

……...

(Chairman, Department Graduate committee) signature

Dr. Shimeles Fisseha

……...

Advisor signature

Dr. Elias Lewi

……...

Internal examiner signature

Dr. Getenet Mewa

……...

External examiner signature

ACKNOWLEDGEMENTS

First and foremost I am grateful to my advisor Dr. Shimeles Fisseha for the proper supervision, support and guidance he provided me throughout my research. His critical comments, brotherly approach and unreserved effort have given me the opportunity to explore more. I sincerely appreciate his patience and willingness to devote much of his time and energy at all stages of my work. I would also like to extend my acknowledgments to Dr. Tigistu Haile for his helpful comments and sharing valuable resources, time and support during my field work. My thanks also go to Dr.Gezahegn Yirgu for sharing me important reference materials, and to department and staff members of Earth Sciences and Geophysical observatory to their unlimited cooperation.

My gratitude also goes to Ethiopian Geological Survey for letting me to use all the necessary materials and data with all its staff members especially to Geophysics department for their invaluable assistance to use computer softwares. Special thanks to Dr. Getnet Mewa, Ato Moges Tigabie, and Ato Befekadu Oluma.

I have no words to express my special thank to my friend and brother Alemayehu Gartew at St. Mary's University College for giving me his personal laptop during my research work. I also extend my heart felt thank to all my staff members, collogues and friends at St. Mary' University College for their invaluable moral support. I appreciate and thank St. Mary's University College for arranging me off time during the two years study.
I am also grateful to my friend Shibru Temesgen lecturer at Addis Ababa University for his unreserved support.

Last but not least, my deepest heart felt gratitude also goes to my family. Their care and encouragement has played important role throughout my academic life.

TABLE OF CONTENTS

LIST OF FIGURES

ABSTRACT

In this thesis work three integrated geophysical investigations namely; gravity magnetic and electrical resistivity sounding have been carried out over Gemeto thermal springs. The area is situated in the central sector of the main Ethiopian rift at a close proximity to the SE of Awassa town.

The study aims at investigating all the necessary geothermal characteristics in the area based on the thermal manifestations. To achieve the objectives of the research, the required data for each of the geophysical method applied in this study are collected, processed, and interpreted .Based on the results obtained from the data analyzed using standard softwares; interpretations and concluding remarks are also given.

Results from gravity survey indicate two interesting features; the first one is the heat source for the Gemeto thermal springs has been characterized. Small area near the springs has shown uniquely the lowest negative Bouguer anomaly values. In principle, lowest Bouguer anomaly values are indicatives of either high cliffs or high density materials. Our study area is inside the Awassa caldera where high density volcanic rocks are common with the lowest topography in the area. Therefore, the lowest Bouguer anomaly values in the area are interpreted as densities of rocks in the area are lowered due to thermal expansion. The second one is the regional structural trend extending NE-SW that is clearly shown on the Bouguer and regional anomaly map. Interpreted as an extension and integral structure of the eastern escarpment of the rift.

From the magnetic anomaly map, the area proposed by the gravity method to be the possible heat is also characterized by the lowest total magnetic field response. This is interpreted as rock units in that area are forced to lose their elements with magnetic properties due to high temperature. The method has also shown different major shallow

fault structures mainly lying in NNE-SSW and N-S directions. The 2-D magnetic models prepared along two profiles also confirm these results.

Results from vertical electrical soundings along one profile show that the first top layer up to 10m has resistivity values of 2-24 Ω m which is indicative of alluvium soil deposits in the area and the second layer of thickness between 20 to 60m, the resistivity value varies from 12-37 Ω m which is interpreted as coarse clay materials. In both geoelectric and pseudosection diagram shallow structure between VES3 and VES4 is observed which is interpreted as one of the major shallow structures identified by magnetic method. These shallow structures identified by magnetic and electrical methods are possible structures that recharge the area.

Based on the joint analysis of these geophysical methods and thermal manifestation, the area has the potential for small scale development such as center for recreation and thermal therapy. Besides, additional geophysical methods are proposed to further reinforce the outcome of the study.

CHAPTER ONE

1. INTRODUCTION

1.1. Background

Geothermal Energy is the energy contained in intense heat that continually flows outward from deep within Earth. This heat originates primarily in the core.

The inner part of the Earth is divided into three layers, namely the innermost layer (core), the middle layer (mantle) and the outermost layer (crust). The earth's core lies almost 6437.4 km beneath the earth's surface. The double layer core is made up of very hot molten iron surrounding a solid iron in the center. The temperature of the core is estimated to range from 4000 to 5000 ^{o}C. Surrounding earth's core is the mantle, thought to be partly rock and partly magma. The mantle is about 2900km thick and temperatures in the mantle may reach 3700 °C.

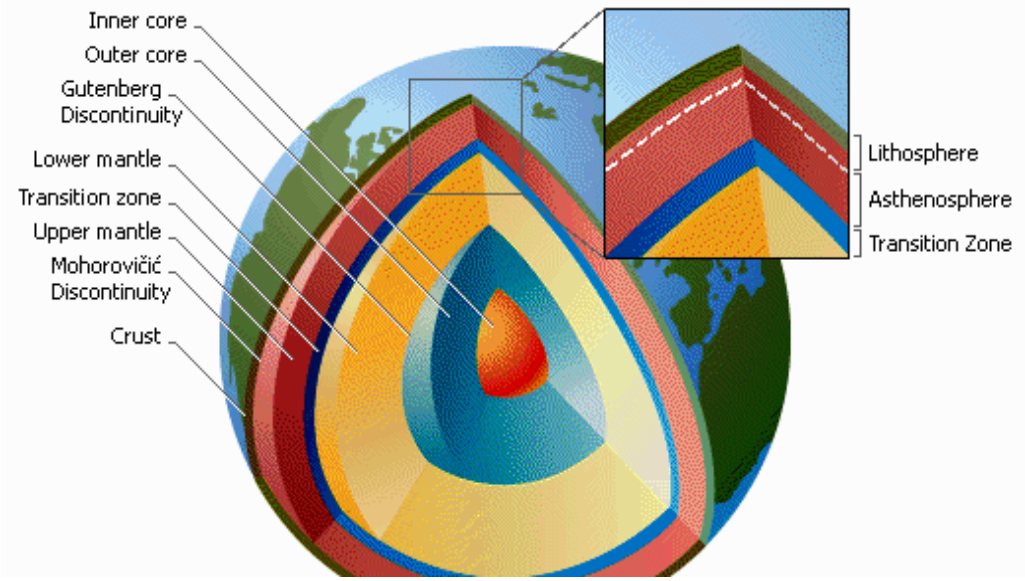

Figure1.1 Internal structure of the Earth, [Microsoft Encarta, 2006]

The outermost, brittle layer of the earth, the lithosphere, is not one continuous sheet of rocks, but is broken into pieces called plates. These slabs of continents and ocean floor drift apart and push against each other in the process called plate tectonics. This process can cause the lithosphere to become folded, faulted (cracked), fractured or thinned, allowing plumes of magma to rise up in to the crust. The convective (circulating) motion in the mantle drives plate tectonics the "drift" of Earth's lithospheric plates. Where plates spread apart, molten rock (magma) rises up into the rift (opening), solidifying to form new crust. Where plates collide, one plate is generally forced beneath the other (subducted). As the subducted plate slides slowly downward into the mantle's ever-increasing heat, it melts, forming new magma. Plumes of this magma can rise and intrude into the crust, bringing vast quantities of heat relatively close to the surface. If the magma reaches the surface it forms volcanoes, but most of the molten rock stays underground, creating huge subterranean regions of hot rock.

The magma can take from 1000 to 1,000,000 years to cool as its heat is transferred to surrounding rocks. In certain areas, water seeping down through cracks and fissures in the crust comes in contact with this hot rock and is heated to high temperatures. Some of this heated water circulates back to the surface and appears as hot springs and geysers. However, the rising hot water may remain underground in areas of permeable hot rock, forming geothermal reservoirs. Geothermal reservoirs, which may reach temperatures of more than 350° C (700° F), can provide a powerful source of energy.

There is abundant geothermal energy in the earth's crust and it has the potential to make the energy economies of many countries through out the world particularly as fossil fuels grow more expensive and scarce. Geothermal energy is known as a renewable energy source because the water is replenished by rainfall, and the heat is continuously produced with in the earth by the slow decay of radioactive particles that occur naturally in all rocks. It is also known to be of those less pollutant energy sources. Interest in renewable energies has increased recently due to environmental problems associated with

conventional energy sources. It is generally accepted that the emission of greenhouse gasses from fossil fuels causes global warming and declining air quality. Renewable energies generally don't cause pollution or cause greenhouse gas emission.

The Ethiopian rift is branded with tremendous geothermal potential. The Rift is characterized by high tectonic activity, where magma bodies are injected into the continental crust where fracturing is common. Due to these features, the Rift is an area where excess heat flow is supported by additional geological and hydrogeological factors to result in surface manifestations of the heat. Fracturing may also result in the escape of some of the heat to the surface, thus providing direct indications of the presence of a hydrothermal system. These features make the rift a high geothermal potential. Of this great potential, however, a little is studied and utilized; the Aluto geothermal field and the Boku thermal centre are relatively well studied in the MER. Further studies need to be carried out since there are areas where geothermal potentials are manifested in the main Ethiopian Rift, MER.

One of the least studied and un-utilized of the many thermal springs, despite its close proximity to growing city centers like Awassa is the system of thermal springs at Gemeto. The geothermal springs of Gemeto are large discharge superheated thermal water springs found between the Awassa Town and Wendo Genet thermal Centers with recorded spring temperatures in excess of 80°C. Local people are currently using the thermal waters for religious and thermal therapy purposes. There is a minimal development of the potential in the form of local infrastructure, access road, etc. And one also rarely finds literature and material devoted to the study of this resource whose occurrence seems to be an integral part of the Awassa collapsed caldera system.

This research was planned to carry out integrated geophysical survey around the springs to study the thermal centers, their surface extent, discharge volume, temperature, structural controls of the field, the potential sources of recharge and possibly its

discharging mechanism. The study is also expected to show the relationship between the hot springs and the nearby Awassa caldera as a possible source of the necessary heat, and the Awassa and Shallo Lakes and the surrounding surface water bodies in relation to their role in providing the necessary recharging water to sustain the large discharge volume from the springs.

1.2. Location of the study area

The study area, Gemeto, is found in the central sector of the Main Ethiopian Rift, MER (fig.1.2). It is about 275km south of Addis Ababa, close (about 5km) southeast of the Awassa town. The area lies within the geographical coordinate of 6^0 50'- 7^0 20' North and 38^0 20'- 38^0 50' East latitude and longitude respectively.

Off the main asphalt road, the study area can be accessed by a dirt road which may require a four-wheeled drive vehicle during the rainy seasons. The topography can be described as flat with small isolated hills (volcanic domes).

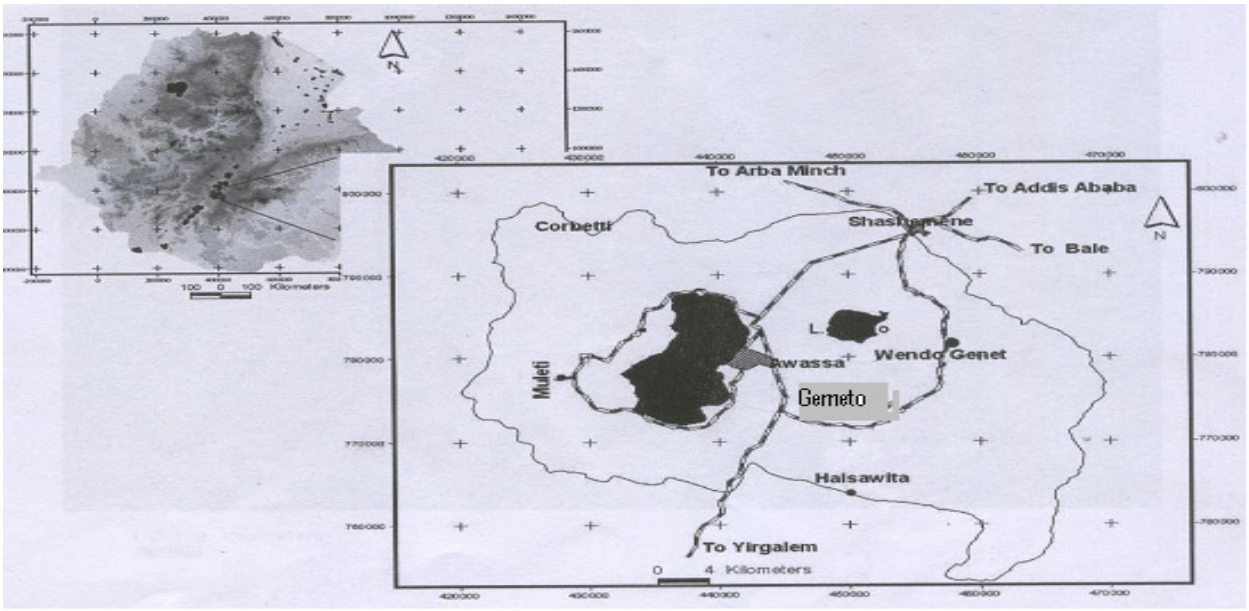

Fig.1.2 Location map of the study area (Modified after Wondwosen Mokonnen,2005)

1.3. Research objective(s)

The main objective of the integrated geophysical survey around the springs is to characterize the thermal and hydro-geological setting of the thermal centres. This requires a multi-disciplinary approach and immensely helps to understand their surface extent, discharge volume, temperature, structural controls of the thermal field and potential sources of recharge and possibly discharging mechanism.

The results of this study is thought to provide the necessary background information for small scale development of the thermal springs for using the resource as resort, thermal therapy centre, etc… .

The geophysical work carried out at the study area specifically aims to determine:

- the role of the nearby Awassa caldera in terms of providing the necessary heat source
- the influence of surface water bodies, such as lakes Awassa and Shallo in providing the required recharge waters to sustain the high discharge volume of the springs,
- Mapping the major geological structures in the vicinity of the spring and asses their role as paths for rising hot waters and the recharging conduit of the springs,

1.4. Methodology

Although the setting of a geothermal field is mainly controlled by the regional geology, its local characteristics, such as its manifestation at the surface through a geothermal system, are essentially hydrogeological phenomena. They depend not only on suitable heat source but also on the presence of a medium (normally water) in which the heat can be transported to the surface and on a permeable path along which the medium (the fluid) can travel. In simple terms, the recipes for a geothermal system are: large source of heat,

a reservoir to accumulate heat, a barrier to hold the accumulated heat and adequate supplies of water (ancient connate, magma waters or more recent juvenile, meteoric waters). A good understanding of these components and their interaction is essential for better utilization and development of the resource. A successful exploration program, therefore, should be directed at studying and resolving these components.

This research plans to integrate existing surface geological and hydrogeological maps and other relevant information with subsurface geophysical investigations in order to study the component parts directly or indirectly.

The gravity method would helps to map regional geological structures in the area. The magnetic method would map the major structures that are paths for the rising heat to shallow depths to interact with the down flowing waters in the aquifer zone. The deep electrical sounding surveys would establish the vertical stratification of the geoelectric layers of the area

1.5. Structure of the Thesis

This thesis is organized in to five chapters. The first chapter is general introduction of the study. The second chapter discusses previous geological works of the MER as well as the study area. The third chapter addresses the theoretical backgrounds of the geophysical methods employed in this study. In the fourth chapter, compilation of the different maps and models and their qualitative and quantitative descriptions are presented. The fifth chapter presents conclusions and recommendations of the work. Lastly reference materials used for this work are listed alphabetically.

CHAPTER TWO

2. GEOLOGICAL AND TECTONIC REVIEWS

2.1. Geological and Tectonic reviews of the main Ethiopian rift.

Volcano–tectonic activities during the Cenozoic had played significant roles for the development of the present day Ethiopian Rift system. The Ethiopian rift system is part of great East African rift system, widely believed to have been formed by diverging lithospheric plates, which is active since the early tertiary times. The Ethiopian Rift system is commonly used to designate the three discreet rift segments namely, the Afar depression, the Main Ethiopian Rift (MER), and the Southern Ethiopian Rift (SER). The Great east African rift itself is part of the Afro-Arabian rift system that extends for about 6500km (Mohr, 1962) from Turkey in the north to Mozambique in the south passing through the Red sea, Eritrea, Ethiopia, Kenya, Tanzania, and Malawi.

The Main Ethiopian Rift (MER), about 80km wide is the central segment of the Ethiopian rift system. It extends in a NE/NNE to SW/SSW direction from the southern Afar rift (9º30') to Konso highland (5º15') in southern Ethiopia. Based on structural features, the MER is divided into three geographic segments represented by the northern (Fen tale- Nazareth), central (Nazareth- Awassa), and southern (Awassa–Konso) sectors. The central sector, where the study area belongs to, is a symmetric rift basin where both sides of the rift margins are fully defined except in the region between Guraghe and Sodo of the western escarpment and in the Shashemene area of the eastern margin.

The Guraghe Mountains and the Agere-Selam fault scarps of the western and eastern rift margins respectively expose stratigraphic sections that are more than a kilometer in

thickness. Thick volcanic sequences also occur in the Omo & Wabshebele river canyons on both sides of the rift shoulders (G. W/Gabriel & Aronson, 1987; G. W/Gabriel 1990).

There is no universal agreement as to when the Ethiopian rift system begins to develop. Different Authors have given different dates (Backer et al., 1972, Meyer et al., 1975, Kazmin, 1979, Kazmin et al., 1980).Burke and Dewey, (1970) relate the development of east African rift system to the afro-Arabian doming in the lower tertiary time. On the other hand, (Mohr, 1967; Behet, 1979; Mcconnel et al., 1980) described the Afro-Arabian rift system is an expression of a tectonic zone of weakness in the lithosphere, which dates back to Precambrian. However, the actual development of the rift is agreed to have commenced at the end of the Mesozoic or the beginning of the tertiary.

Following the Mesozoic era there was extensive magmatism and faulting which modified the face of east Africa. Faulting was accompanied by widespread volcanic activity.
The wide spread late Eocene uplift in the Ethio-Arabian region, indicated by rapid marine regression, which is considered to be the formation of the Eastern rift system uplift and axial down-wrapping .In Ethiopia these phases where preceded and accompanied by outpouring of the Eocene–Oligocene trap series fissure basalts. Mohr (1971b) recognized three main episodes of swell uplift in Ethiopia; in the late Eocene, middle Miocene, and late Pliocene-early Pleistocene. Trap volcanism in Ethiopia was related to the earliest stage of the uplift. It was during the last uplift that the Main Ethiopian Rift (MER) was faulted to its present form.
The formation of the MER is attributed to extensional tectonics (Mohr & Behere, 1978), though the direction of relative motion between blocks (extensional direction) is still controversial. According to (Wolde Gabriel et al., 1990), the development of the rift has been episodic rather than continuous, and – a two stage rift development is proposed based on structural and stratigrafic relationship from the central sector of the MER. The

initial stage was characterized by the development of a series of half grabens along the rift with alternating polarity (in late Oligocene, early Miocene and early Pliocene times). Accordingly the same workers believe in the evolution of the rift from alternating half graben to full symmetrical graben with a medially located neovolcanic zone that is bifurcated to marginal garbens in the northern sector of the MER.

The MER is characterized by a great number of faults which produced a total altitude of more than 1500m (Di Paola, 1972) between the top of the plateau and the floor of the rift. The style of faulting within the MER is dominated by NNE trending swarms of en-echelon tensional faults which commonly produce horsts and grabens. All these faults are normal step faults of various dimensions and throws mainly along NNE-SSW and rarely along NE-SW, N-S and NW-SE directions (Mohr, 1967, Di Paola, 1972).The Wonji Fault Belt (WFB) is the youngest structural deformation, largely concentrated within a narrow, 5-12km wide belt of normal faults in the Ethiopian rift valley that is characterized by NNE-SSW oriented fault zone and running through the whole length of the MER. The WFB is forced into en-echelon transpositions in order to remain with in the rift margin envelop (Mohr, 1980). These sites of transpositions are characterized by very recent and closely spaced normal faults, extensional fractures (Chorowicz et al., 1994) and other faults related open structures with significant volumes of fissural basalts related differentiation products of very recent age and even historical (Di Paola,1976). These structures are considered to be important for ground water circulation and controlling the drainage system of the rift floor. In the central sector of the MER, where our study area belongs the WFB is right laterally offset into four en-echelon rift-axis segments.

The rift floor is covered by Mio-Pliocene to present volcanism (basalt, trachaytic and rhyolitic lavas, and pyroclastic flows and falls), and volcano sedimentary products (Abate and Saggri, 1979). Most part of the floor of MER is covered by silicic pyroclastic materials, mainly per alkaline rhyolitic ignimbrites, interlayered with basalts and tuffs

associated with un-welded pumice (Mohr, 1962, Di Paola, 1972, Weldegebriel et al., 1990). They are early to middle Pliocene. Alkaline and Per-alkaline rhyolitic lava flows associated with pumice and ash represent the late silicic volcanic events (Di Paola,1972) where they were erupted from late Pliocene and middle Pleistocene, and in some places outcrop as remnants as large caldera. As summarized by G. Wolde Gabriel et al., (1990) most of the geological sections exposed along the rift margins are dominated by tertiary volcanic rocks except for a few locations where crystalline basement is unconformabilly overlain by Mesozoic marine sedimentary and/or tertiary volcanic rocks.

2.2. The geological framework of the study area.

As described above the MER is divided in to three sectors; among these three sectors the one where our research interest belongs to is found in the central sector. The central part of the rift is asymmetrical both morphologically and stratigraphically. The lowest part of the floor lie close to the eastern escarpment, and are occupied by lakes. Seven lakes of tectonic and volcano tectonic origin occur on the rift floor. From south to north they are Chamo, Abaya, Awassa, Shalla, Abijata and Ziway. Lakes Shalla and Awassa have no outlets.

Lake Awassa must have a comparatively rapid turnover time, losing water by underground seepage, because its waters are not highly mineralized in comparison with lake Shalla's water (Zemenu Germew, 2000). The Awassa basin, where the study area is located is found in the central sector of the MER and is a depression- a large caldera (25 to 30km in diameter) which was generated by volcano- tectonic collapse phenomena. This caldera is composite; containing the younger 15km wide nested corbetti caldera within its southern margin. It is bounded by all sides by high and steep fault escarpments (Mohr, 1962; 1967; Di Paola, 1972; Geze, 1974; Raunet, 1974).

Lake Awassa (analyzed, NB-37/2/47), approximately 1780m a.s.l., occupies an unusual tectonic basin completely enclosed by faulting, in the Ethiopian rift south of corbetti volcanic center. It covers about 125km2 and comparatively shallow but, in common with other lakes in the region has recorded since the Pleistocene. The ancient lake Awassa covered a much larger area, particularly to the east where it flooded a swampy "plain", now occupied in the north by Lake Shallo. Hot springs emerge in this "plain" and on the escarpment of the east.

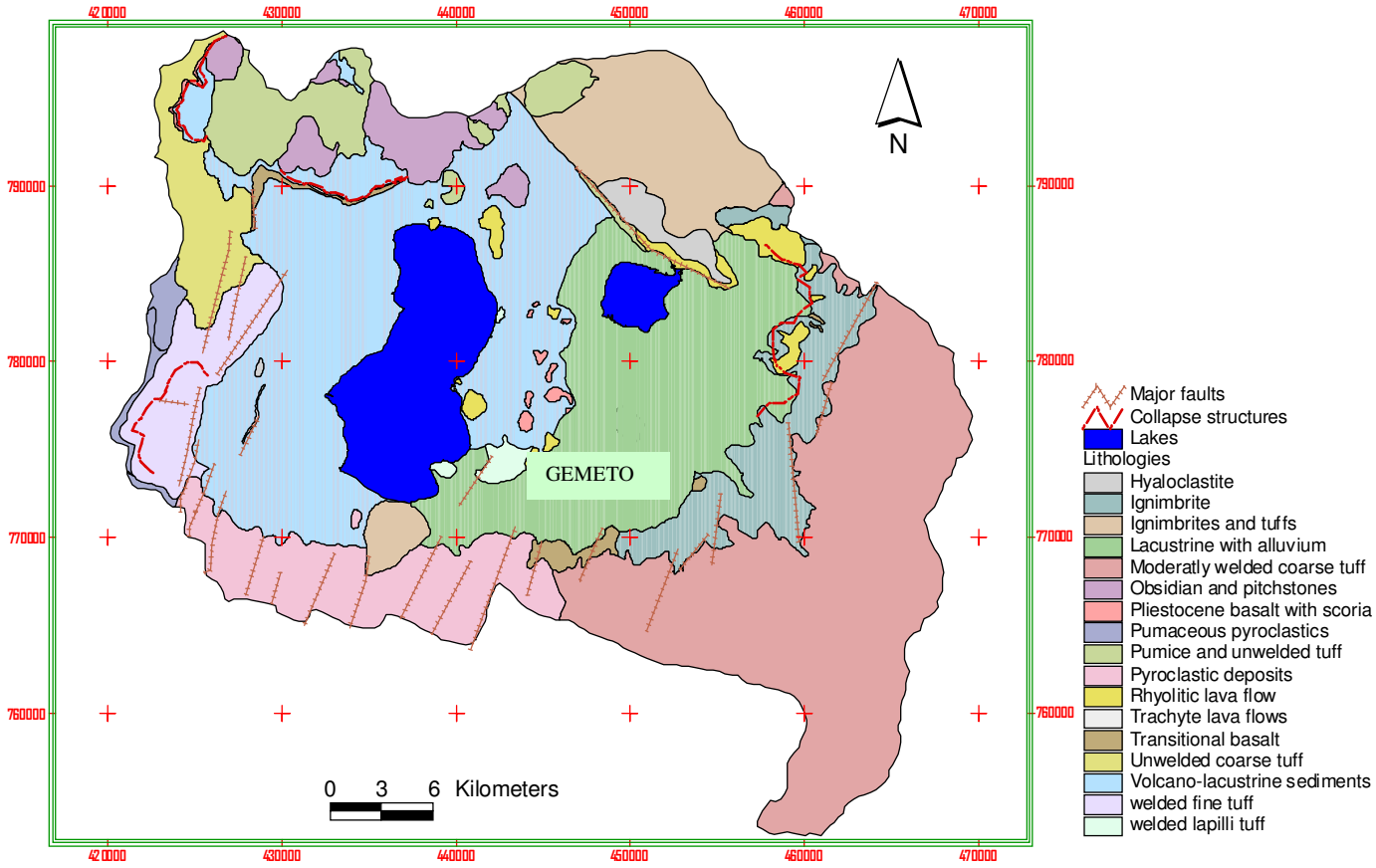

Fig.2.1 Geologic map of Gemeto and its surrounding
(Modified after Zenaw Tesema, 2003)

Regional structures limited the size of the ancient lake- in the N-E by a major east west

fault downthrown south, in the south by a lofty traverse escarpment downthrown north, and in the east and west by the fault blocks bounding the Ethiopian rift. West of the Shashamane-Awassa highway the scarp is buried beneath sediment, ignimbrite, and young pyroclasties, but east of the road it gains topographic expression eastwards. Basaltic tuffs were mapped near the top of the scarp, but the bulk of the rocks where shown as rhyolites,and farther east near the eastern escarpment of the rift, a large rhyolitic volcano, collapsed on the south west was recognized as a caldera (Di Paola, 1970, pp.21) on the floor which the fertile Wondogenet farm is located.

The main Awassa caldera is asymmetrically overlapped and displaced against the eastern rift escarpment causing this rift margin arcuate, while corbetti is along the rift axis. These calderas only slightly eroded walls are relatively young features along the eastern marginal graben of the rift floor. More than 500m of mostly air fall ash and ignimbrite are exposed in the caldera wall against the eastern escarpment (Gidey Wolde Gabriel, 1987). However, the northern and southern walls of the main caldera are subdued perhaps due to rifting and burial along the MER. The north-eastern wall of the Awassa caldera is poorly defined, though a NW-SE fault (Werencha fault) has exposed the stratigraphic successions.

The western wall of the Awassa caldera, i.e. the Abaya ridge, is well preserved and affected by the regional faults, WFB, running NNE-SSW. The floor of the caldera is mostly covered by lake Awassa and Shallo plus a marshy area. However, numerous smaller volcanic structures also occur with in the caldera. South of the Awassa town a remnant of what is probably an old rhyolite edifice rises above the plain.

It is composed of rhyolites with layers of obsidian flow, tuff or pumice breccia and ignimbrites covered a layer of hyaloclastites all of which deep south and terminate abruptly on the north at an arcuate, eroded escarp. It is suggested by some workers (UNDP, 1973, Tesfaye Korme et al., 1997) that this scarp marks the edge of a Cauldron subsidence. It is also suggested that the swampy plain east of Awassa occupies an old

caldera as indicated by the arcuate arrangement of young extrusions with in the caldera (UNDP, 1973).

The floor of the caldera is also highly dissected by the normal faulting especially to its southern and western side. Normal faults running in NE-SW (N200E) direction with down throws up to 100m are clearly visible cutting the young pyroclastic and lacustrine deposits. In the southern side of lake Awassa, a traverses escarpment with a northly down thrown is clearly evident, which has limited the size of the ancient large lake. Faults may act either as path ways for water movement or as flow barriers. At the foot of some of the faults which bounded the basin there exist springs, hot and cold indicating that these faults act as conduits. Faults at the floor may possibly be filled with a weathered glassy volcanic ash and as a barrier.

The occurrence of differently oriented fractures is also noted in the caldera floor. Fractures running in N10^{o}E to N60^{o}E and N100^{o}E to N115^{o}E are evident especially on the flat topped hyaloclastites. The former group is dominant and run for longer distances than the later which is infrequent and short. Most of the fractures are widely spaced, 0.5m, filled and form irregular blocks. These fractures, especially the former ones may be signatures of the effect of the western plateau.

The occurrence of deep-seated extension fractures in the study area is reported by Tesfaye Korme et al., (1997). According to these workers, the rhyolite ridge in the south east side of the Awassa town is a type-B volcanic neck. These ridges are short and steep hills of trachytes and/or rhyolite lava necks commonly associated with the calderas and are of the result of ejection of volcanic materials into radial and annular fractures formed by pressure exerted by the magma chamber. Their trends don't necessarily coincide with the strike of extension fractures in the region. It is suggested from their arrangement that, the young basaltic cinder cones of 1.52± 0.06Ma age (Mohr, 1980) distributed in the

caldera floor may be similar injections in to fractures. Columnar joining is also observed in the ignimbrite beds located in the NW-SE transfer fault area on the north eastern and southern sides of Lake Awassa.

All the various types of geological (structural) features, especially the boundary faults, are thought to play a significant role in the recharging and circulation of water within and possibly out of thermal systems within the study area.

CHAPTER THREE

3. THEORETICAL BACKGROUNDS IN GEOPHYSICAL METHODS

3.1 Introduction

In exploration Geophysics, there are different geophysical methods that respond to the physical properties of the sub-surface media. These geophysical methods can be classified into two broad groups. The passive methods, those that detect variation within the natural fields associated with the earth; such as gravitational and magnetic fields. And the active methods, those that use artificially generated sources such as electrical methods, seismic methods and others. As it is clearly stated on the preceding chapter, chapter one this research plans to carry out an integrated geophysical survey through using magnetic, gravity and electrical methods.

Generally speaking, the gravity method is used in mapping regional geological structures. The magnetic and the gravity methods are known to complement each other and therefore the magnetic method is also used in mapping large scale geological structures. The electrical resistivity methods would help to map the local structures and establish the vertical stratification of the geoelectric layers in the study.

3.2 THE GRAVITY METHOD

3.2.1 Introduction

The gravity method is a passive geophysical method that measures variation in the earth's gravitational field caused mainly by difference in the density of the sub-surface rocks. The gravity method is a potential field method that is based on the earth's gravitational field. This method is used in modeling the earth's crustal structures, in locating areas of anomalous mantle materials (in areas of plate margins) and it is the basis for the study of the earth's shape (Telford, 1990). The method of gravity survey in geophysics involves measurement, reduction, mapping, and interpretation of gravity data (Dobrin, 1988). Gravimetry is the method of measuring and modeling the gravity field of the earth (Torge, 1989).

3.2.2 Fundamental Principles

The bases of gravity survey lie on the two physical laws, Namely; Newton's law of universal gravitation, and Newton's second law of motion. The first of these two laws states that the force of attraction between two particles of known mass is directly proportional to the product of the two masses and inversely proportional to the square of the distance between their centers of mass. This statement is mathematically given by the equation:

$$F = \frac{-Gm_1m_2}{r^2}\,\hat{e} \qquad (3.1)$$

Where, F- is the mutual force of attraction between m_2 and m_1

G - is the gravitational constant which is equal to $6.67 \times 10^{-11} m^3/kg.s^2$

$\hat{e}$ – is a unit vector whose direction is the line connecting the centre of the two masses.

r - is the distance between the two masses m_1 and m_2.

From Newton's second law of motion the force, F is the product of mass, m and acceleration, a; the acceleration of m_2 is given by:

$$F = \frac{-Gm_1m_2}{r^2}\hat{e} = m_2a \qquad (3.2)$$

:

For the case of the earth of mass M_e and a body of mass, m located on or in the vicinity of its surface:

$$F = \frac{-GM_em}{r^2}\hat{e} = mg \qquad (3.3)$$

From the above equation (eq.3.3);

$$\vec{g} = \frac{GM_e}{r^2}\hat{e} \qquad (3.4)$$

g – is gravity or gravity acceleration. The unit of 'g' is Gal in the honor of Galileo Galili. 1 Gal = 1 cm $/s^2$. In geophysics we also use auxiliary units like milliGal. (mGal), micro Gal and so on. But the mGal unit commonly used; $1mGal = 10^{-3} cm/s^2$.

3.2.3 Theoretical Gravity of the Earth

Considering a small mass, m moving with a velocity, ν on the surface of the earth rotating with angular velocity $\vec{\omega}$, it is possible to develop the theoretical gravity or the normal gravity value of the earth .

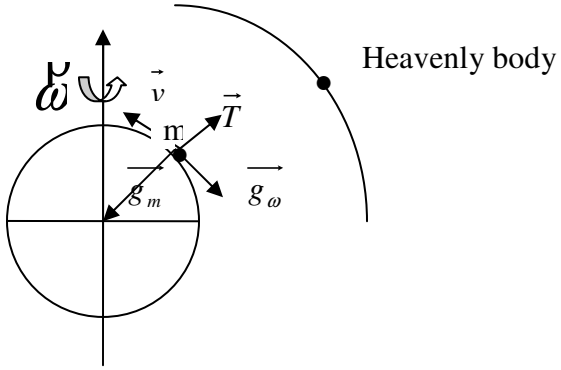

Fig 3.1. Modeling Gravity (gravity force per unit mass acting on a mass, m on earth)

Where $\vec{g}_m$ - attraction force per unit mass acting on m due to earth's mass

$\vec{g}_\omega$ - Centrifugal force per unit mass acting on m due to earth's rotation with $\vec{\omega}$

T- is Tidal force per unit mass acting on m due to mass attraction of other heavenly bodies.

The resultant force per unit mass acting on m is;

$$\vec{g} = \vec{g}_m + \vec{g}_\omega + \vec{C} + \vec{T} \qquad (3.5)$$

Where C is Coriolis force per unit mass acting on m due to its motion and its value is zero if m is at rest on the earth's surface.

If we assume the earth to be spherical in shape with radius R;

$$\vec{g}_m = \frac{GM}{R^2}\,\hat{e}\,; \text{ and } \vec{g}_\omega = \vec{\omega}(\vec{\omega} \times \vec{R}) \qquad (3.6)$$

The effect of C and T on $\vec{g}$ is usually considered negligible in actual work. Therefore, gravity $\vec{g}$ refers to the combined effect of both earth mass gravitation and rotation

$$\vec{g} = \vec{g}_m + \vec{g}_\omega, \text{ or } \vec{g} = \frac{GM}{R^2}\hat{e} + \vec{\omega}(\vec{\omega} \text{x} \vec{R}) \qquad (3.7)$$

3.2.4 The Major Forces Acting on a Body on the Earth's Surface.

Assume a spherical shape earth rotating with angular velocity, $\vec{\omega}$ and a small mass resting on earth's surface as shown in the figure below.

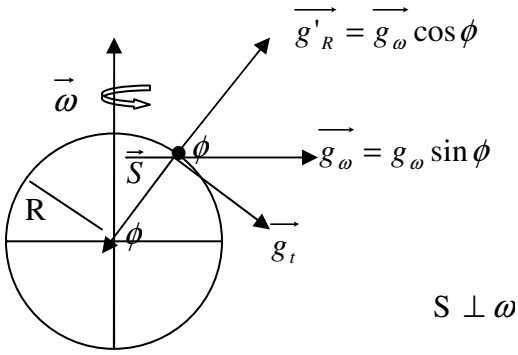

Fig. 3.2 components of forces acting on mass, m on earth's surface

From the figure above the force acting on mass m placed on the earth's surface are: g_m (attraction force per unit mass due to the earth's mass M) and $\vec{g}_\omega$ (rotational force per unit mass due to the earth's rotation). The resultant gravity force per unit mass on mass, m will be taken from eq. (3.7)

$$\vec{g} = \vec{g}_m + \vec{g}_\omega \qquad (3.8)$$

From figure 3.2, the following relations are clearly shown.

$$\vec{S} = \text{Rcos}\phi \tag{3.9a}$$

$$\vec{g}_{\omega} = \omega^2 \text{S} = \omega^2 \text{Rcos}\phi \tag{3.9b}$$

$$g'_R = \vec{g}_{\omega} \cos\phi = \omega^2 \text{ R cos}^2\phi \tag{3.9c}$$

$$g'_t = \vec{g}_{\omega} \text{ Sin}\phi = \omega^2 \text{ R Sin}^2\phi \tag{3.9d}$$

This implies that;

$$\text{g} = \text{g}_\text{m} - g'_R = \frac{GM}{R^2} - \omega^2 \text{ R cos}^2\phi \tag{3.10}$$

Where- g'_R is the radial component of $\vec{g}_{\omega}$.

and g'_t which the tangential component of $\vec{g}_{\omega}$ has no effect on mass, m.

Therefore; eq (3.10) will be reduced into

$$\text{g} = \frac{GM}{R^2} - \omega^2 \text{ R cos}^2\phi \tag{3.11}$$

- At the equator ($\phi = 0^0$)

$$\text{g} = \text{g}_\text{e} = \frac{GM}{R^2} - \omega^2 \text{ R cos}^2 0^0$$

$$\text{g}_\text{e} = \frac{GM}{R^2} - \omega^2 \text{ R} \tag{3.12}$$

- At the pole ($\phi = \pm\ 90^0$)

$$g_p = \frac{GM}{R^2} - \omega^2\ R \cos^2 90^0$$

$$g_p = \frac{GM}{R^2} \qquad (3.13)$$

From equations (3.12) and (3.13) one can conclude that gravity value, g is minimum at the equator and maximum at the poles; but for the real earth observed values of gravity, g at the poles and equator are g_p= 983.218 Gals and g_e = 978.032 Gals respectively. The difference between g_p and g_e yields about 5.2 Gals (g_p-g_e= 5.2 Gals) and calculations on a theoretical basis for a spherical earth model is about 3.4 gals (g_p-g_e = ω^2 R =3.4 Gals). The disagreement between observed values of gravity g for a real earth and calculated value of gravity, g for a spherical model earth is due to the assumptions used above. From these disagreements one can conclude that;

- The shape of the real earth is not spherical.
-The shape of the earth is rotationally distorted one such that its shape is flattened at the poles and bulged at the equator.
- Gravity value, g varies as a function of latitude, ϕ

3.2.5 The Geoids and the Reference Ellipsoid

Geodesist and geophysicists consider two surfaces that represent the average shape of rotationally distorted real earth to study its gravity field, shape and size. These are the geoid and the reference ellipsoid

a). The Reference Ellipsoid.

An idealized geometrical or mathematically generated theoretical earth model flattened at the poles and bulged at the equator. This model of the earth assumes no undulations on the earth's surface where as we have hills, mountains and depressions on the real earth. It also considers only radial variations in density of the earth plus centrifugal acceleration. A theoretical earth model up on which the variation of gravity, g with latitude (ϕ) is computed according to an international agreements in 1967 by IUGG as:

$$\gamma = g_e (1 + C_1 \sin^2\phi + C_2 \sin^2 2\phi) \qquad (3.14)$$

Where $g_e = 978.0490$, C1 =0.0052884 and $C_2 = -0.0000059$

b).The Geoid

A physical surface on earth referred to the mean sea level that must be related to the reference ellipsoid for its practical work. The geoid is a practical surface on which g values observed on the actual to topography of the real earth are mathematically shifted to its surface using gravity reduction methods which we are going to discuss later. Unlike the references ellipsoid, the geoid shows wide undulations following topography of real earth. And also the geode considers both radial and lateral variation in density of the earth and centrifugal acceleration.

3.2.6 Gravitational potential

Gravitational fields are conservative, that is to say, the work done moving a mass in a gravitational field is independent of the path traversed and depends only on the end

points. In fact if the mass is eventually returned to its original position the net energy expenditure is zero, regardless of the path followed.

The gravitational force is a vector whose direction is along the line joining the centers of the two masses. The force giving rise to a conservative field may be derived from a scalar potential.

$$\nabla U(r) = g(r) \qquad (3.15)$$

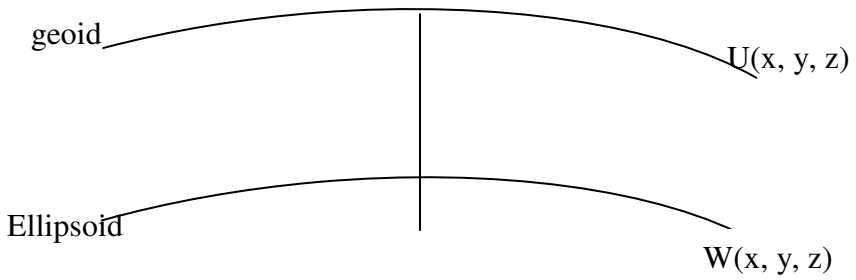

Fig 3.3 diagram representing potential surfaces of geoid and ellipsoid

Where W(x,y,z) and U(x,y,z) are the ellipsoid and geoid potentials respectively.

Assume that the earth's gravity potential at a point on the geoid at a point on the ellipsoid are equal to the same constant, U_o.This assumption leads to the fact that the ellipsoid and the geoid are both equipotential surfaces that fit each other at mean sea level. This idea can mathematically be expressed as:

$$U(x, y, z) = W(x, y,z) = U_o \qquad (3.16)$$

$\frac{\partial U}{\partial z}$ = g_o - Gravity observed on the geoid surface

$\frac{\partial W}{\partial z} = \gamma$ - Theoretical gravity computed on the ellipsoid surface using the theoretical gravity formula;

And finally the formula to find theoretical gravity value, g at any point on the ellipsoid was adopted by International Union of Geophysics and Geodesy in 1967, as:

$$\gamma_{1967} = 978.0490\ (1+ 0052884\sin^2\phi + 0.000059\ \sin^2 2\phi\ ) \quad (3.17)$$

Having all these information gravity anomaly, Δg can be written as:

$$\Delta g = g_o - \gamma \quad (3.18)$$

Where, g_o is observed gravity value of a certain station.

3.2.7 Gravity Reductions

The gravity g values that we determine by gravity surveying are different from place to place on the actual surface of the earth all over the world. The readings will generally be influenced by latitude, tidal effect and instrumental drift, elevation and topography. To reduce them to the value they would have on some datum equipotential surface such as the geoid, or surface every where parallel to it, some adjustment is important. The following are important components of gravity data reduction; free air correction, Bouguer correction, Terrain (topographic) correction latitude correction and drift correction.

I. Latitude Corrections: - Both the rotation of the earth and its slights equatorial bulge produce an increase of gravity with latitude. The centrifugal acceleration due to its spinning earth, maximum at the equator and zero at the poles- opposes the gravitational acceleration while polar flattening also increases gravity at the poles (Telford, 1990).

As indicated in chapter one, our study covers very small area which leads us to consider latitude correction insignificant Therefore, this research ignores latitude correction.

II. Free Air Correction: - The free air correction is based on the fact that the attraction of the earth as a whole can be considered to be the same as if it's mass where concentrated at its center. Hence, it is necessary to correct the readings so that all the field readings are reduced to a datum surface. The correction factor for free air correction has been calculated as:

$$\delta g_{FA} = 0.3086 \text{hmGal/m} \qquad (3.19)$$

Where h is the topographic height above sea level.

Note that the free air correction is added to the gravity readings when the station is above the geoid and subtracted when below it.

III. Drift Correction: - this accounts for time dependent mechanical changes within the gravimeter. One can find out how gravimeter readings change with time by graphing frequent readings made at the same location with times of these readings. To determine both tides and drift effects properly, one should make gravimeter readings at one to three hours intervals. (Robinson, 1988).

Note that positive drift requires negative correction and vise versa.

IV. Bouguer Correction: - The Bouguer correction accounts for attraction of material between the station and the datum plane, which was ignored in the free air calculation.

If the station were centrally located on a plateau of large horizontal extent and uniform thickness and density of gravity readings would be increased by the effect of the slab between the station and the datum plane.

The Bouguer correction, derived by assuming the slab to be of infinite horizontal extent is given by:

$$\delta g_B = 2\pi \ G\rho h \tag{3.20}$$

where h is the height of the gravity station above the geoid and G is the gravitational constant and ρ is the density of the material for mean crustal density (ρ = 2.67gm/cm^3) and h in meters, the Bouguer correction reduces to:

$$\delta g_B = 0.1119h \text{ mGal. /m} \tag{3.21}$$

The Bouguer correction is applied in the opposite sense to free- air correction. It is subtracted when the station is above the datum plane and vice-versa.

V. Terrain Correction:- This correction accounts for surface irregularities in the vicinity of the station, that is hills rising above the gravity station and valleys (or lack of material) below it. Both topographic features affect the gravity measurement in the sense, i.e. reducing the readings due to upward attraction by the excess mass of hills or mass deficiency (less attraction) due to valleys. Terrain corrections are, therefore, always positive and always added to the station reading. There are several graphical methods for calculating terrain corrections. All of them require a good topographical map of the area.

3.2.8 Gravity Anomalies

When all of the preceding corrections have been applied to the observed gravity reading, we obtain the value of Bouguer gravity. The Bouguer anomaly is the difference between the measured value at the point of observation and theoretical value calculated for that elevation or water depth by considering a Bouguer slab of appropriate density for the effect of the earth's material between the geoid and the station ;eq. (3.18)
The Bouguer anomaly calculated by ignoring topographic effects is known as simple Bouguer anomaly (S.B.A).

$$S.B.A = g_{obs} + 0.3086h - 01119h - \gamma \quad (3.22)$$

When all the corrections, the free air, Bouger and terrain corrections are applied to the observed gravity, the resulting anomaly obtained by subtracting the standard theoretical gravity at the given latitude is known as the complete Bouger anomaly (C.B.A)

$$C.B.A = g_{obs} + 0.3086h - 01119h + \delta g_t - \gamma \quad (3.23)$$

Where, δg_t is the terrain correction factor.

3.3 THE MAGNETIC METHOD

3.3.1 Introduction

The magnetic method of geophysical prospecting is also a passive potential method. It measures earth's magnetic field caused by difference in the susceptibility of the sub-surface rocks. The magnetic method is the oldest of the geophysical methods of locating both hidden

ores and structures, such as faults and fractures associated with deposits of oil and gas. An example of this is in petroleum exploration, where magnetic method is used to identify faults in the basement that may control the depositional history of the sedimentary basin. Magnetics have also been used in the magnetic anomalies associated with hydrothermal alteration which have been used in geothermal exploration, as mapping of the magnetization contrast at the Curie transition. (Berhanu Mengistu,1999).

Although magnetic and gravity methods are the two potential methods that have some properties in common, there are some basic differences between this two methods. One example of all these is that precise interpretation of magnetic field data is much more complex than for gravity. And also other differences and similarities between these two methods are always written on many geophysics books.

3.3.2 Principles and Elementary Theory

Like the gravity method, the magnetic method is also a potential field method in which its initial defining parameter is the magnetic force. The expression for magnetic force is obtained from Coulomb's law for magnetic poles and mathematically given by:

$$\vec{F} = \left(\frac{m_1 m_2}{\mu r^2} \right) \mathbf{r}_1 \qquad (3.24)$$

Where, F- is the magnetic force

m_1 and m_2- are the magnetic poles

r- is the separation distance between the two poles.

$\mathbf{r}_1$- is a unit vector directed from m_1 to m_2

μ **-** is the permeability of the medium surrounding the magnets.

A more practical quantity than the force F is the strength of the magnetic field existing at a point in space, as a result of poles strength m located at a distance r from it. The magnetic field strength, H is defined as the force on a unit pole:

$$H=\frac{\vec{F}}{m'}=\left(\frac{m}{\mu r}\right)\mathbf{r}, \qquad (3.25)$$

Where m' is a fictitious pole at the point in space and is in effect the instrument of the measurement.

Magnetic poles always exist in pairs, so the fundamental entity is the magnetic dipole, two poles of strength, -m and +m separated by a distance λ. Therefore, the magnetic moment is defined as:

$$M= m\lambda r_1 = \mu r_1, \qquad (3.26)$$

Where, M is a vector in the direction of the unit r_1 extending from –m towards +m.

A magnetic body placed in an external magnetic field becomes magnetized by induction. The intensity of magnetization is proportional to the strength of the field and its direction is proportional to the strength of the field and its direction is in the direction of that field. It is defined as the magnetic moment per unit volume, that is,

$$I=\frac{M}{V}= \text{£}_i r_1 \qquad (3.27)$$

Where, £_i is the induced polarization.

Practically this magnetization by induction amounts to lining up the dipole of the magnetic material; for this reason I is often referred to as the magnetic polarization. If I is constant and has the same direction throughout, the body is said to be uniformly magnetized.

The degree to which the body is magnetized is determined by its magnetic susceptibility, defined as:

$$\kappa = \frac{£}{H}, \qquad \text{or} \qquad I = \kappa H \tag{3.28}$$

Susceptibility is the fundamental parameter in magnetic prospecting; since the magnetic response of the rocks and minerals is determined by the amount of magnetic materials in them in them and latter have k values much larger than the rock and the minerals themselves.

In a medium with magnetic susceptibility k with in the body of the earth where magnetizable materials exists the total magnetic field within the body is given by:

$$B = H + H' = H + 4\pi I \tag{3.29}$$

The proportionality constant, $1+ 4\pi \kappa$ is equivalent to the permeability, μ. Thus equation (3.28) can be written as,

$$B = (1+4\pi \kappa) H \tag{3.30}$$

By definition the ratio of induction B to magnetizing force H is the magnetic permeability, μ thus may be written as:

$$B = (1 + 4\pi \kappa) H = \mu H \tag{3.31}$$

The permeability is a measure of the modification by induction of the force of attraction or repulsion between two magnetic poles. Its magnitude depends on the magnetic properties of the medium in which the poles are immersed.

3.3.3 Magnetism of the Earth

In comparison with other geophysical data relating to the earth, the amount of information accumulated for the geomagnetic field is relatively enormous. As far as exploration geophysics is concerned, geomagnetic field is of three parts. These are: the main field, the external field, and variations of the main field.

I. Main Field, which although not constant in time, varies relatively slowly and is of internal origin.

A. Elements of earth's magnetic field.

At any point along the earth's surface, a magnetic needle free to orient itself in any direction around a pivot at its center will assume a position in space determined by the direction of the earth's magnetic field F at that point. Normally this direction will be at an angle with north south direction. The magnitude of this field, F, the inclination of the needle from the horizontal, I, and its declination, D, the angle it makes with the geographic north, completely define the magnetic field. The different magnetic elements are illustrated in the figure shown below:

The seven parameters, X, Y, Z, D, I, H and F, known as the magnetic elements, are related as follows:

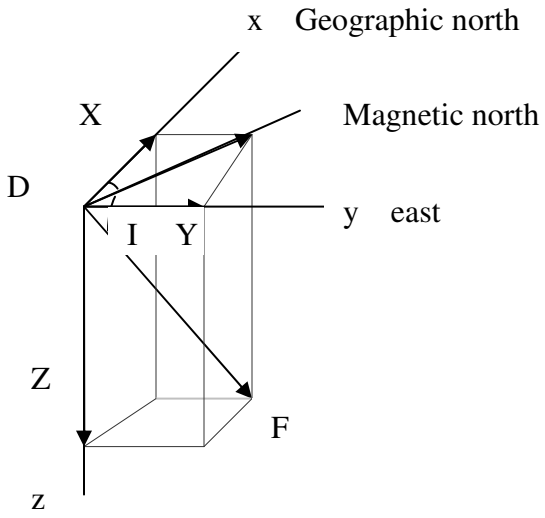

Fig.3.4 Elements of the earth's magnetic field

$$\left.\begin{aligned} &F^2 = H^2 + Z^2 = X^2 + Y^2 + Z^2, \\ &H = F\cos I, \quad Z = F\sin I, \qquad \tan I = Z/H \\ &X = H\cos D, \; Y = H\sin D, \qquad \tan D = Y/X \end{aligned}\right\} \qquad (3.32)$$

H, Z, D magnetic elements recorded at geomagnetic observatories

Lines of equal declination, inclination, horizontal intensity, etc., when plotted on maps, are called isomagnetics charts. They show the variations in the geomagnetic field over the earth's surface.

B. Origin of the Main Field

The main geomagnetic field theoretically could be caused by an internal or external source, either of permanent magnetism or of unidirectional current flow, or it could be the result current flowing in and out of the earth's surface. The latter possibility can be ruled out because of the observed air to earth currents are much too small to account for the existing

magnetic field of the earth. Spherical harmonic analysis of the observed surface magnetic fields show that at least 99% are due to sources inside, the remaining 1% to sources outside the earth.

The present theory is that the main field is caused by the electric currents circulating in the outer core known to be liquid from seismic evidence which extends from a radius of 1300km to 3500km. the magnetic source is thought to be a type of self exited dynamo, in which a highly conductive fluid moves about in complex mechanical motion, while electric currents possibly by chemical or thermal variations, flow through it. The combination of motion and currents creates a magnetic field. Since little is known, or is likely to be known, the earth's core, the theoretical development is difficult. Laboratory tests have shown, however, that the dynamo source may be a valid explanation and also that it may account for certain slow or secular variations which are known to have occurred in earth's magnetic field.

C. Secular Variations

Slow changes in the earth's field which take place progressively over decades or centuries are known as secular variations. Such changes are noted in all the magnetic elements at magnetic observatories everywhere in the world. The rates of change vary with time.

The projection of currents rates of secular variation is not reliable means of determining past fields of predicting futures ones. Paleomagnetic observations show that there have been variations as well as repeated reversals of the earth's field over geological time, the most recent one taken place in a very short time. The mechanism for the reversals is not well understood, although most theories associate it with changes in the flow of electric currents within the earth which are induced by conducting material in the earth's core set into motion by convention.

II. The External Magnetic Field: A small variations of the main field (about1%) which varies rather rapidly, partly cyclically and partly randomly and which originates outside the earth, appears associated with electric currents in the ionized layers of the outer atmosphere. The variation in time is much more rapid than for the so- called permanent field. Several well documented effects are listed below.

a. **A cyclic of 11 years duration**, corrected with sun spot activity, has a latitude distribution which indicates an external origin
b. **Solar diurnal variations** with a period of 24 hours and range of 30 γ, vary with latitude and season and are probably controlled by action of the sun on ionosphere currents.

c. Lunar diurnal variations of 25 hours period and amplitude of about 2 vary cyclically through the month and seen to be associated with a moon ionosphere interaction.

d. Magnetic storms:- in addition to the predictable short term variations in the earth's field, there are transient disturbances which by analogy with their meteorological counterparts are called magnetic storms. Such storms cause considerable disruption in magnetic prospecting operations. The oscillations that take place while they are going on are so rapid and unpredictable that it usually is not feasible to correct for them as with diurnal variations. Magnetic surveys must generally be discontinued during storms of any severity.

III. variation of the main fields (local anomalies): usually but not always much smaller than the main field, relatively constant in time and place and caused by local magnetic anomalies in the near surface of the earth, these are the targets in

magnetic prospecting. Important changes occur in the main magnetic field as the result of variations in the magnetic mineral content of near surface rocks.

These anomalies are occasionally large enough to double the main field locally. In general they do not persist over very great distances, that is to say, magnetic maps do not exhibit large scale regional features, such as isostatic anomalies in gravity.

3.3.4 Magnetic Data Reduction

Measurements (magnetic, gravity etc) are normally made at a regular or random intervals along a grid or otherwise selected paths whose locations are noted for subsequent plotting.

Corrections (diurnal correction, δB) are applied to the measured values (B_{obs}). The dipole field determined from International Geomagnetic Reference Field (IGRF) maps is subtracted from the measurements acquired at each station to generate magnetic anomalies as:

$$\Delta B = B_{obs} \pm \delta B - B_D \qquad (3.33)$$

The profiles when plotted should be smoothly varying and expressive of anomalies of interest. If there is an excessive amount of such geologic or magnetic noise (anomaly), at a wavelength much shorter or much longer than is of interest, it is possible to apply simple filtering techniques to facilitate interpretation of the profile.

3.5 The Electrical Resistivity Method

The electrical resistivity method is one of the different geophysical exploration methods that utilize artificial sources. This method is based on the natural variation of the resistivities of sub-surface soil and rock formations.

The large contrast in resistivity between ore bodies, fluid inside rocks, alteration mineral assemblages and their host rock is exploited in electrical resistivity prospecting. It is used to map lithologic layers and unique geologic structures. (Tibebu A, 2001).

In electrical resistivity method, a direct, accumulated or low frequency alternating current is introduced into the ground by means of two electrodes; while potential between two points on the ground is measured by other two point electrodes called potential electrodes. The sub-surface rock resistivity variations affect the electrical current flow that affects the distribution of surface rock resistivity variations affects the distribution of the surface electrical potential. Deviation from the pattern of potential difference expected from a homogeneous ground provides information on the form of the sub-surface anomalous mass that is referred to as resistivity anomaly (Parasnis, 1989).

The potential difference for unit current sent into the ground is the measure of electrical resistance of the ground between the measuring terminals. This resistance is a function of geometrical configuration of the electrodes and the electrical parameters of the ground.

3.5.1 Fundamental Principles of the Method

Measurements of electrical resistivity are made with circuits in which the earth is one of the components, namely, a resistor. The physical principle underlying the electrical resistivity method is embodied in Ohm's law. Assuming a continuous current flowing in an isotropic homogeneous medium. If ΔA is an element of surface and J the current density, then the current passing through ΔA is $J\Delta A$. The current density J and the electrical field E are related through Ohm's law as:

$$J = \sigma E \tag{3.34}$$

Where E is in volts/meter and σ is the conductivity of the medium in mhos/meter.

The electric field is the gradient of scalar potential,

$$E = -\nabla V \tag{3.35}$$

Where V is in volts. Thus we have

$$J = -\sigma \nabla V \tag{3.36}$$

After considering some necessary conditions, one can reach on Laplace's equation, i.e. the potential is harmonic:

$$\nabla^2 V = 0 \tag{3.37}$$

Mostly two electrodes are used to supply a controlled electrical current to the ground. Such electrodes are called current electrodes. From the two current electrodes, there is a set of successive equipotential surfaces, in the form of a hemispherical surface. The potential difference between the equipotential surfaces can be measured where they intersect the ground surface using a second pair of electrodes called potential electrodes.
Consider an electrode of small dimensions buried in a homogeneous isotropic medium. The current circuit is completed through another electrode, usually at the surface placed at infinite distance or at least at far distance so that its effect is negligible.

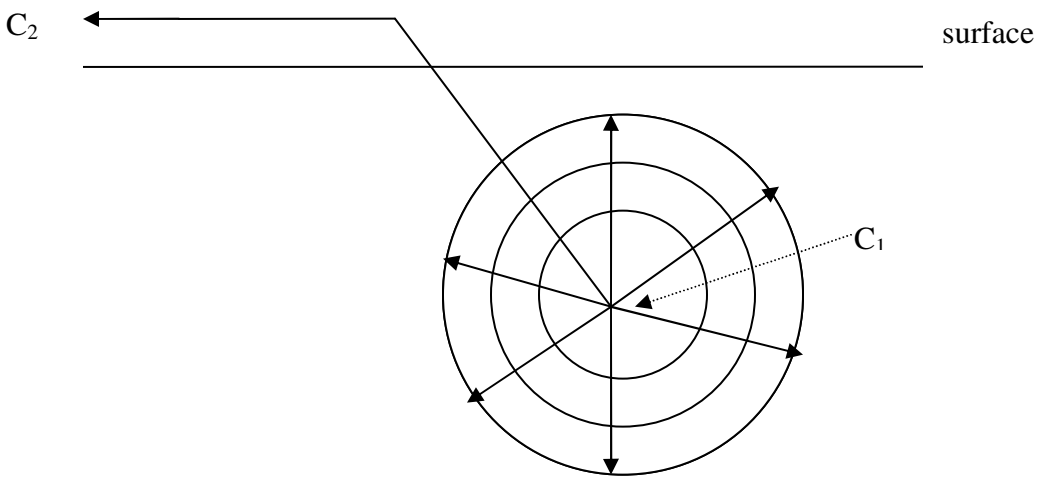

Fig 3. 5 buried point source of current in a homogeneous ground.

As shown in the above figure, the current lines will be directed radially outwards from the source.

From the symmetry of the problem, the potential will be a function of only the radial distance 'r' from the source electrode. Under this conditions Laplace's equation, in spherical coordinates, simplifies to:

$$\nabla^2 V = \frac{1}{r^2}\frac{\partial}{\partial r}\left[r^2 \frac{\partial V}{\partial r}\right] = 0$$

Or

$$\nabla^2 V = \frac{\partial^2 V}{\partial r^2} + \frac{2}{r}\frac{\partial V}{\partial r} = 0 \qquad (3.38)$$

Multiplying throughout by r^2

$$r^2 \frac{\partial^2 V}{\partial r^2} + 2r \frac{\partial V}{\partial r} = 0 \tag{3.39}$$

Integrating both sides of the equation,

$$\int \frac{\partial^2 V}{\partial r^2} + 2r \frac{\partial V}{\partial r} \partial r = 0 \tag{3.40}$$

This implies that

$$\frac{\partial V}{\partial r} = -\frac{A}{r^2} \tag{3.41}$$

Integrating equation (3.40) once more

$$V = -\frac{A}{r} + B \tag{3.42}$$

Where A and B are integration constants

Boundary conditions

1. As $r \to \infty, V \to 0, B = 0$

2. the total current flowing through a sphere of radius r

$$I = 4\pi r^2 \vec{J}, \ \bar{J} = -\sigma \bar{E} = -\sigma \frac{\partial V}{\partial r} = -\sigma \frac{A}{r^2}$$

$$= 4\pi r^2 \left(-\sigma \frac{A}{r^2} \right)$$

So that

$$I = -4\pi\sigma A \Rightarrow A = -\frac{I\rho}{4\pi}$$

Where $\sigma = \frac{1}{\rho}$ is the resistivity of the homogeneous layer.

Therefore, the potential

$$V = \frac{I\rho}{4\pi}\left(\frac{1}{r}\right) \quad \text{Or}$$

$$\rho = 4\pi r\left(\frac{V}{I}\right) \tag{3.43}$$

In the case when a current source is placed on the surface, all the current now flows through a hemispherical surface in the lower medium. Therefore, equation (3.42) will be divided by two and will take the form:

$$V = \left(\frac{I\rho}{2\pi}\right)\frac{1}{r}, or \rho = 2\pi r\left(\frac{V}{I}\right) \tag{3.44}$$

This leads to the formula for the ground resistivity to any electrode configuration.

The electrical resistivity of the ground as measured by two potential electrodes after current is introduced to the ground by two other current electrodes is:

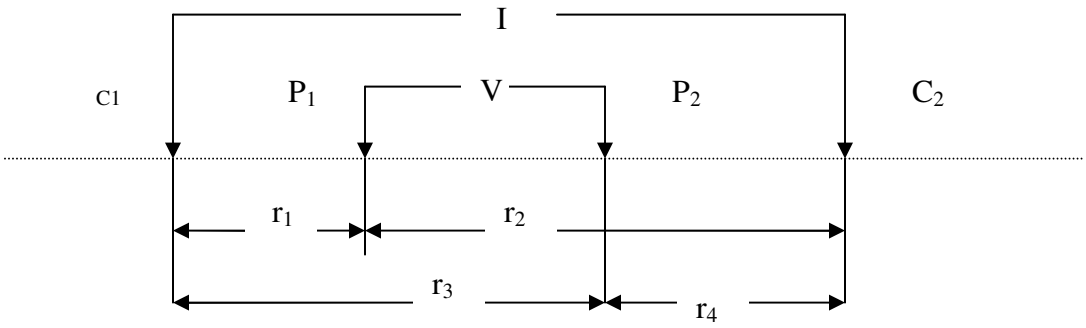

Fig. (3.6) two current and two potential electrodes on the surface of homogenous isotropic ground of resistivity ρ (After Telford, 1990)

From the diagram electrical resistivity of the ground surface can be derived as:

The potential at point P_1 is;

$$V_{p1} = \frac{I\rho}{2\pi}\left[\frac{1}{r_1} - \frac{1}{r_2}\right] \tag{3.45}$$

And the potential at P_2 is;

$$V_{p2} = \frac{I\rho}{2\pi}\left[\frac{1}{r_3} - \frac{1}{r_4}\right] \tag{3.46}$$

The potential difference between P_1 and P_2, ΔV will be:

$$\Delta V = V_{p1} - V_{p2}$$

$$\Delta V = \frac{I\rho}{2\pi}\left[\left(\frac{1}{r_1} - \frac{1}{r_2}\right) - \left(\frac{1}{r_3} - \frac{1}{r_4}\right)\right] \tag{3.47}$$

Or

$$\rho = 2\pi\left\{\frac{1}{\frac{1}{r_1}-\frac{1}{r_2}-\frac{1}{r_3}+\frac{1}{r_4}}\right\}\left(\frac{\Delta V}{I}\right) \tag{3.48}$$

$$\rho = K\left(\frac{\Delta V}{I}\right) \tag{3.49}$$

Where K is the geometric factor

The resistivity determined would have been true resistivity if the ground were homogeneous and isotropic. However, usually the ground constitutes various materials

and there might be some variations in the lateral or vertical dimensions and the resistivity determined is called apparent resistivity

The apparent resistivity measured depends not only on the nature of the geologic formation but also on the geometric dispositions. And hence Equation (3.48) will be modified as:

$$\rho_a = K\left(\frac{\Delta V}{I}\right) \tag{3.50}$$

Where ρ_a is the apparent resistivity.

There are several styles of electrode arrangements for resistivity survey. These are the Schlumberger array, the Wenner array, pole-dipole array, dipole-dipole array and others.

This study utilizes the Schlumberger array. Therefore, in the next sub- section we will discuss this configuration in depth.

3.5.2 The Schlumberger Array

The Schlumberger array is the symmetrical arrangement in which the points A,M,N and B are taken on a straight line such that the points are symmetrically taken about the center of the spread (sounding point),O. When this arrangement is used for sounding, the separation is kept constant for a number of AB values, which are successively increased for larger depth penetrations. Nevertheless, when the value of MN, in comparison to AB, becomes too small the potential difference drops significantly, to be measured precisely, it needs to be increased accordingly.

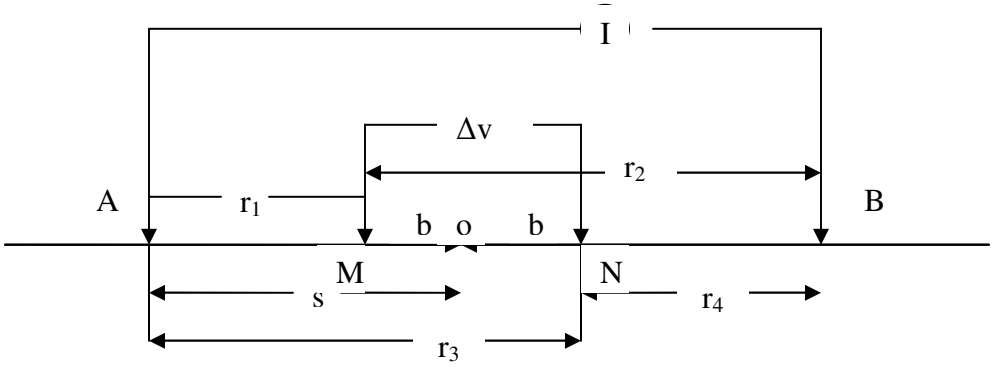

Fig.3.7 Electrode spreads in Schlumberger array.

From fig.(3.7) one can observe the following relations.

$$r_1 = s - b, \quad r_2 = s + b, \; r_3 = s + b, \quad r_4 = s - b$$

Substituting the above relations in to equation (3.47) and operating the mathematical relations;

$$\Delta V = \frac{I\rho}{2\pi}\left(\frac{2b}{s^2 - b^2}\right) \tag{3.51}$$

Or

$$\rho_{asch} = \pi\left(\frac{s^2 - b^2}{2b}\right)\left(\frac{\Delta V}{I}\right) \tag{3.52}$$

Where ρ_{asch} is apparent resistivity in Schlumberger array.

$\pi\left(\frac{s^2 - b^2}{2b}\right)$ - is the geometric factor in the Schlumberger array.

3.5.3 Field Procedure in Electrical Resistivity Method

Regardless of the specific electrode spread employed, there are only two basic procedures in resistivity work. The particular procedure to be used depends on whether one is interested in resistivity variations with depth or with lateral extent. These two procedures are known as electrical drilling or vertical electrical sounding (VES), electrical profiling, or mapping or sometimes known as lateral inhomogeneity hunter.

I. Vertical Electrical Sounding (VES)

In VES, a set of measurements are taken, at a specific point, such that the value of K is progressively changed resulting in values reflecting the vertical stratification of resistivity in the sub surface, beneath the point of observation. That is why VES is some times known as “vertical electrical drilling”.

Substituting the above relations in to equation (3.47) and operating the mathematical relations;

$$\Delta V = \frac{I\rho}{2\pi}\left(\frac{2b}{s^2 - b^2}\right) \tag{3.53}$$

Or

$$\rho_{asch} = \pi\left(\frac{s^2 - b^2}{2b}\right)\left(\frac{\Delta V}{I}\right) \tag{3.54}$$

Where ρ_{asch} is apparent resistivity in Schlumberger array.

$\pi\left(\frac{s^2 - b^2}{2b}\right)$- is the geometric factor in the Schlumberger array.

Substituting the above relations in to equation (3.47) and operating the mathematical relations;

$$\Delta V = \frac{I\rho}{2\pi}\left(\frac{2b}{s^2 - b^2}\right) \tag{3.55}$$

Or

$$\rho_{asch} = \pi\left(\frac{s^2 - b^2}{2b}\right)\left(\frac{\Delta V}{I}\right) \tag{3.56}$$

Where ρ_{asch} is apparent resistivity in Schlumberger array.

$\pi\left(\frac{s^2 - b^2}{2b}\right)$- is the geometric factor in the Schlumberger array.

By virtue of its relative advantage over other arrays, the electrode configurations widely used in sounding is that of Schlumberger array. In the Schlumberger sounding, the values of MN and the corresponding AB values are chosen in order to get overlapping readings whenever a change over MN values takes place.

II. Electrical Resistivity Profiling

In resistivity profiling or mapping, the values of K remain constant for particular set of readings and measurements are done along a straight line at various points on the surface. In this way, we get the lateral variations of resistivity at a certain depth level.

For such constant depth investigation, the Wenner array is considered convenient due to predefined separations and relative ease in field operation. Moreover, its sensitivity to local inhomogeneities is regarded as a plus sign when employed in profiling surveys.

CHAPTER FOUR

4. DATA ACQUISITION, PROCESSING AND INTERPRETATION

4.1 The Gravity Method

4.1.1 Acquisition and Processing of the Gravimetric Data

The gravity data employed in this study are obtained from the Geological Survey of Ethiopia (GSE), department of geophysics. The data have already been reduced and processed following the appropriate procedures.

The theoretical gravity, γ at latitude ϕ, has been calculated using the 1967 gravity formula (Geodetic reference system 1967; Moritz, 1971). A total of 425 observations are employed for this thesis project and were treated by a homogeneous reference to the IGSN 71 datum. Positions (latitude and longitude) and elevations of the gravity stations are determined by GPS (Global Positioning System) and altimeter measurements.

The Free-air and Bouguer corrections were applied according to the theoretical schemes discussed in the previous sections. A uniform reduction density of 2.67g/cm^3 is used to compute the Bouguer anomalies. The computed Bouguer anomaly corresponds to complete Bouguer anomaly for some stations and simple Bouguer anomaly depending weather or not the terrain correction is taken into account. Therefore, it is the simple Bouguer anomaly that has been considered in this work.

Map presentation and processing, including the separation of regional and residual components from the Bouguer anomaly, were all performed using a “LINUX” script that involves a series of GMT (Generic Mapping Tool) commands.

The regional component is approximated by fitting a lower order polynomial representing a surface. The corresponding residual anomalies were then obtained by removing (subtracting) the above mentioned regional trend from the total Bouguer map.

The distribution of gravity stations, considered under the present study are shown in figure 4.1.

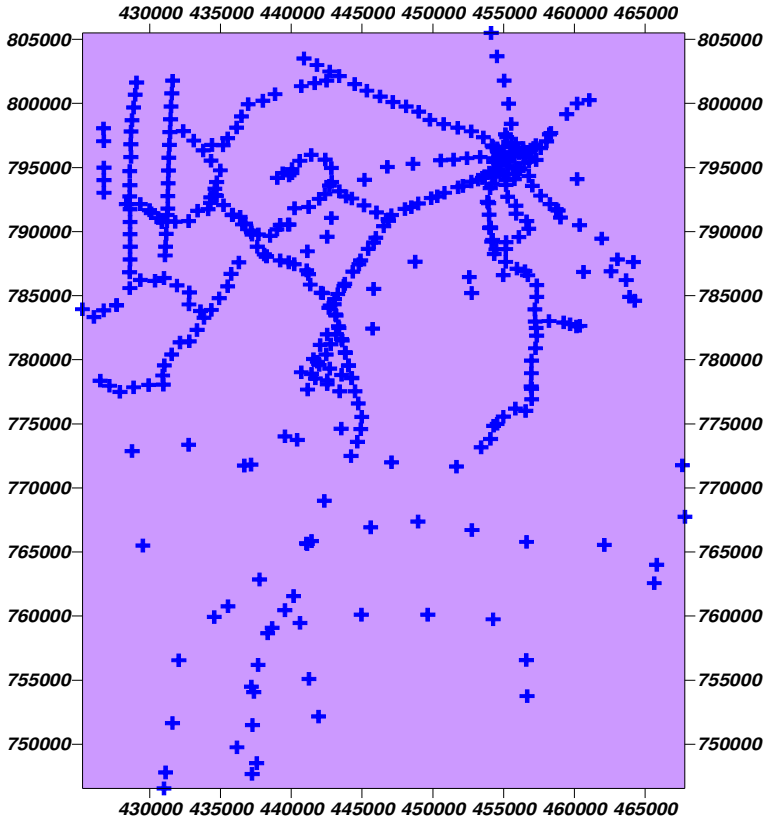

Fig. 4.1, Distribution of gravity stations under this study.

4.1.2 Discussions and Interpretations

The end result of the gravity work in the present study is a compilation of regional gravity anomaly maps that includes the area of interest, using the point gravity anomaly values computed at each observation points. The computed free-air anomaly values are plotted side by side to the point elevation of each station and presented as surface image map in figure 4.2. Bouguer anomaly map (a), the Bouguer regional anomaly map (b) and the Bouguer residual anomaly map (c) are plotted on figure 4.3.

4.1.2.1 Free-Air Anomaly and Topographic Map

The free-air anomaly map and the topographic map (Fig.4.2), clearly exhibits close positive correlations between their respective patterns. The Free-air anomaly map shows its minimum, about -20mGal, in the vicinity of the area of interest, i.e., the region between Awassa and Wondo-genet.

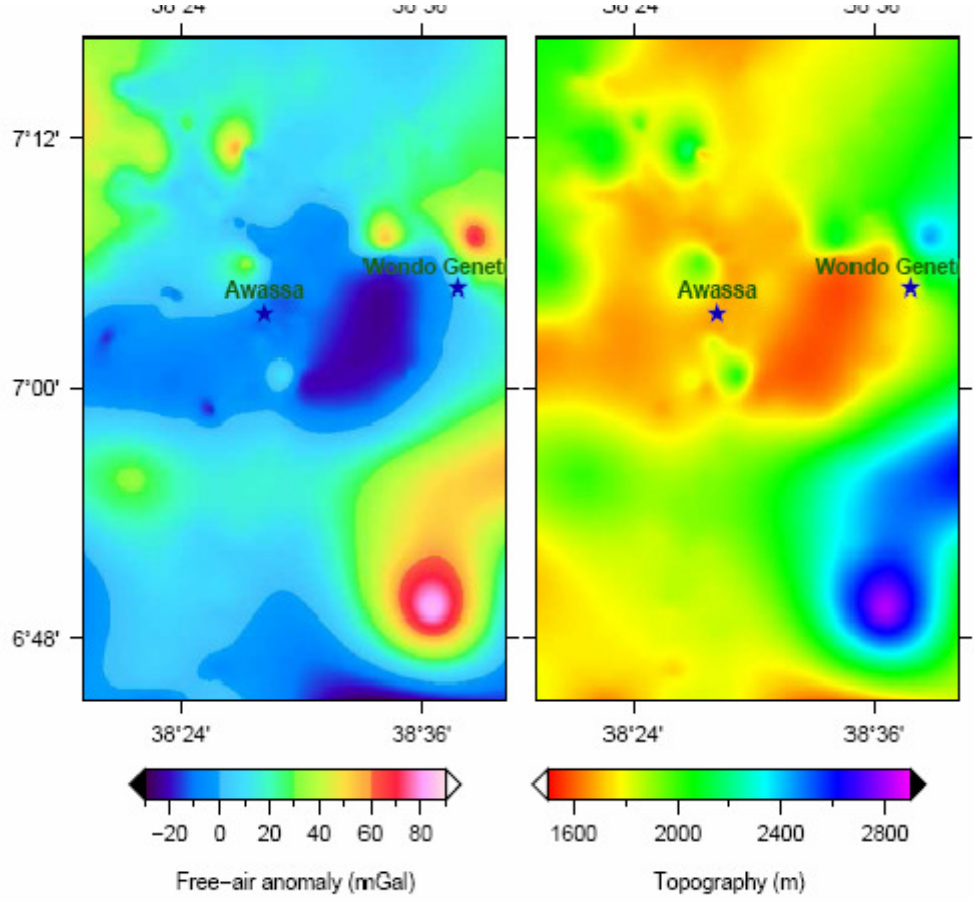

Fig.4.2 Free-Air anomaly and topographic maps of Gemeto and its surrounding

The corresponding region on the topographic map is delineated as local depression designated by lower elevation values of around 1600m. The Gemeto thermal field is part of this region of minimum free-air values and topographic low. A close inspection of the geological map of the region reveals that this anomalous region is dominated by major semi-regional faults and collapsed structures associated to the eastern escarpment of the rift.

4.1.2.2 Bouguer Anomaly Map

The main outcome of gravity work is the Bouguer anomalies, which should correlate with lateral variations in the density of the upper crust. As discussed in the preceding chapter, the Bouguer anomaly is the difference between the observed gravity value, adjusted by algebraic sum of all the necessary corrections and that at some base station, and the theoretical value at the station. On the continental platform, the Bouguer anomaly is generally less than zero and is strongly negative on high mountains. This is due to the mass deficit that exists beneath the continents causing the negative Bouguer anomaly.

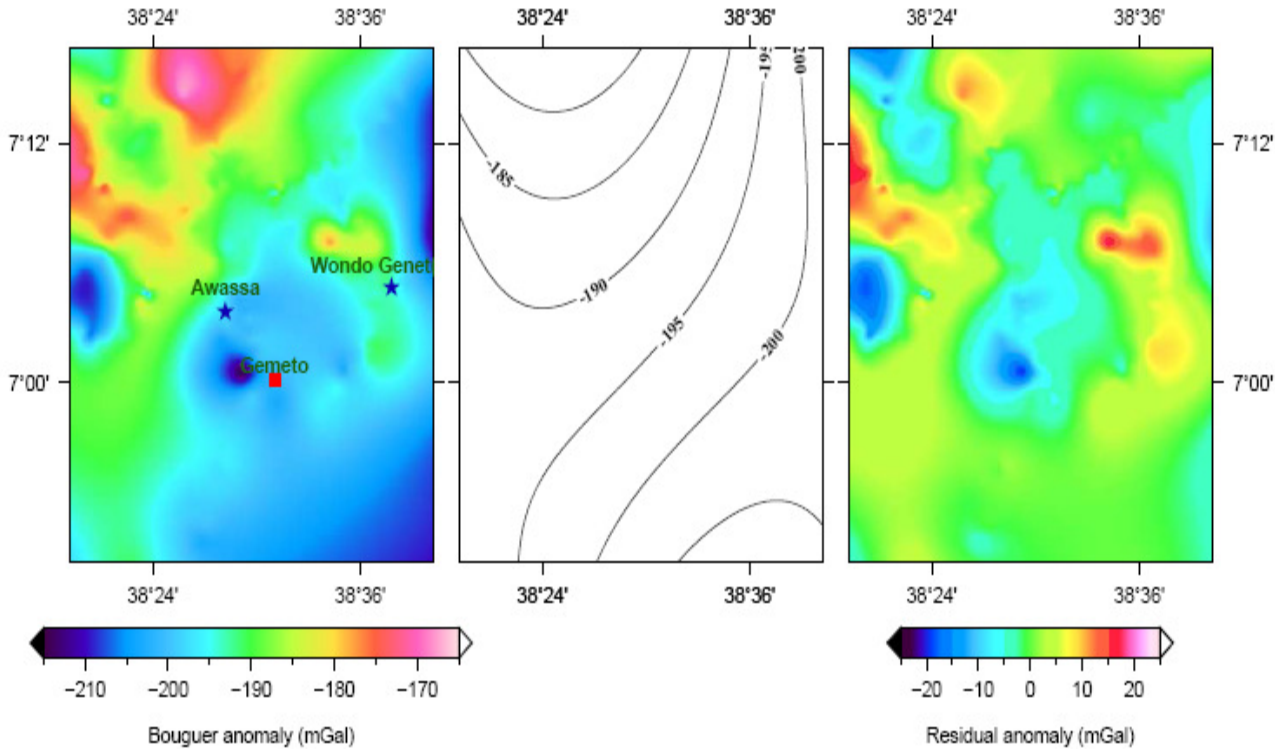

(a) (b) (c)

Fig.4.3 Gravity anomaly maps; a) Bouguer anomaly map, b) Regional anomaly maps c) Residual anomaly map.

Topographic masses shifted to the level below the geoid are not resting on homogeneous crust of constant density or they are not superimposed.

Therefore such gravity anomalies are caused by a change in mass distribution underneath the observation point. These mass distributions could be of shallow or deep origin. Shallow origin mass distributions are subsurface anomalous masses with lateral density variations. Subsurface anomalous masses give rise to negative or positive Bouguer anomalies depending on their density contrast with respect to the mean crustal density ($2.67g/cm^3$) used in the Bouguer reduction. The lateral extent of the Bouguer anomalies due to subsurface anomalous bodies is small compared with those of Bouguer anomalies of deep origin. In general the Bouguer anomalies on local scale are caused by the lateral variation in density of the sub surface masses. On the other hand the non-homogeneous crust of variable density and thickness causes the anomaly on regional scale. On gravity map, the strike of the anomalous subsurface body is the direction of the elongation of the closed curves. High horizontal gradient indicates contacts between rock units of different densities. Steeper gradient indicates shallow contact between rock units of different densities.

The Bouguer anomaly map (fig.4.3a) is generated using the same mapping tool as in the free-air anomaly and topographic maps. The intensity of the Bouguer anomaly in close vicinity of the study varies from a minimum of (-210mGal) around the Gemeto thermal field to a maximum of (-160mGal) to the north and to the north-western part of Awassa town.

Referring to figure 4.3 (a), the Bouguer anomaly in the study area is generally divided into two contrasting zones, by a NE to SW running regional trend. The area west of this boundary is dominated by relatively higher Bouguer values while the area east of the dividing structure, including the study area, generally shows relatively low Bouguer responses. The highest amplitude anomaly values (-170 mGal), within the western zone, are observed to the northern region of the map. Moreover, northwestern part of the Awassa town, is dominated by moderate to-high values (-185 - -175mGal).

This may be interpreted as the effect the high density materials coming from the mantle during the formation of the nearby Corbetti caldera located to northwest of Awassa town. The Corbetti caldera is a nested caldera within the Awassa caldera having elevated volcanic complexes such as Mt.Chebi and Urji with maximum elevation of 2200m.a.s.l.
Around Gemeto, and the surrounding region, including Lake Shallo, the Bouguer anomaly map indicates slow variation ranging between -205 to -200mGal. This may be due to the fact that large part of the eastern Awassa caldera wall is covered by acidic rocks namely, ignimbrites underlying moderately welded coarse tuff. Ignimbrite usually forms low relief flat-topped hills, porphyritic with rock fragments of various size and intercalating weak tuff layers.
Bouguer anomaly also continues to the south of Gemeto with minor variations in amplitude of the anomaly; but the presence of highly dispersed gravity data points and their limited number impose restriction from making meaningful interpretations.

Narrow but strongly negative Bouguer anomalous area (about -210mGal.) is uniquely observed to the southeast of Awassa town. This area represents the Gemeto thermal springs area where a number of local people gather to wash their bodies with the hot water for its thermal healing. The hot water seems “stagnated” forming a “pool” like structure close to the northwestern side of a rhyolite dome on the area. All around the base of this rhyolite dome a number of small hot springs and steams are observed. The cause of this strongly negative Bouguer anomaly may be due to the steam fraction in the high-porosity reservoir rocks as well as to the lowered density caused by thermal expansion.

Area around Wendo genet thermal center indicates relatively higher Bouguer value. The cause of this may be the fact that the area consists mainly of alternating layers of ignimbrites, pumaceous tuffs and volcano lacustrine deposits) interbedded with basaltic lava of probably Tertiary origin (Di Paola, 1972; Raunet, 1974).

4.1.2.3 Bouguer Residual Anomaly Map

Large-scale, deep-seated structures on gravity maps predominate to an extent that it may be very difficult to recognize smaller or shallower features. Therefore, separation of the regional effect to obtain local features is of paramount importance. On this work, the separation of the regional effect from the Bouguer anomaly was performed based on extraction of a trend surface, approximated by a lower order polynomial, representing the so-called regional gravity from the data.

The residual Bouguer anomaly map, (Fig.4.3c), shows the value varies from a minimum of -20 to a maximum of +20mGal. The residual anomaly map has shown much distinctive features from the Bouguer anomaly map which indicates that the effect of the local anomalies were masked by the regional effect. Accordingly, the Gemeto thermal springs and the surrounding swampy plain, extending northeastward including Lake Shallo, is characterized by a gradually rising negative anomalies varying between -10 and 0mGal. Almost the whole of this area is covered with swamps and local geology indicates that this area is covered by lacustrine sediments with alluvium. Similar to the Bouguer gravity anomaly which shows nearly uniform values, the residual anomaly shows the same trend and continuity from Gemeto area up to Lake Shallo. The negative anomalies in this area may be due to low density alluvial, lacustrine sediments, swamps and the effect of Lake Shallo. The small area around Gemeto thermal springs still continues with its lowest anomaly values. This may be due to the effect of heat source on near surface rock units.

Area north and northwest of Awassa town still remains with relatively positive anomalies. The intensity of this positive anomalies show some variation to that of the Bouguer anomaly values. These residual positive anomalies may still be attributed to the Corbetti caldera.

To the east of the Gemeto area a relative positive anomalies extending from N-S direction is clearly observed. These positive anomalies were relatively masked on the Bouguer anomaly map. The N-S extended area exactly represents the eastern escarpment of the rift which includes the known hot springs of Wendo genet recreational center. The positive anomalies in this part of the eastern escarpment of the rift are associated with high density basaltic rocks in the area.

4.1.2.4 Bouguer Regional Anomaly Map

The regional component of the Bouguer anomaly is presented as a contour map with interval of 5mGal, Fig (4.3b). The regional variations that have long wavelength and low amplitude are perceptible over large distances and are thought to be generated by broad crustal structures at relatively deep-seated density contrasts.
Like the total Bouguer map, the regional structural trend follows a NNE-SSW pattern. From the orientation of this regional trend, one can conclude that the overall structural trend is governed by features of the Main Ethiopian rift such as the eastern escarpment.

4.2 Magnetic Method

4.2.1 Instrument, Data Acquisition and Processing.

The instrument used to collect the magnetic data is a proton precision magnetometer (IGS2) which measures the total intensity of the earth's magnetic field. About 250 magnetic data were utilized in this work. The survey has been carried out along many profiles of which (2) profiles are long ones. Of these two profiles used one, (profile1) is approximately along the same line with electrical resistivity survey.

The others are short profiles. The profile directions with their data points are shown in the first magnetic map, Fig (4.4). In addition to the magnetic plan map, 2-D models of the two long profiles have been prepared, Fig (4.5) and (4.6) to enhance the interpretation process. As in the case of gravity, the magnetic anomaly map is prepared using GMT (Generic Mapping Tool) that works in the operating system, LINUX. Regional-Residual separation is performed using the same tool. This regional residual separation was made in order to remove the effect of regional structures and leave local features for which magnetic survey is sensitive to.

The 2-D models of the two profiles are generated with the standard modeling software, GM-SYS, 3.05G.

4.2.2 Interpretation of Magnetic Data

Generally there are two methods of interpreting geophysical data; quantitative and qualitative one. In this thesis work an attempt has been made to make a qualitative appraisal of the magnetic anomaly maps of the study area and 2-D-modeling in order to come up with a quantitative interpretation along two profiles.

4.2.2.1 Qualitative Interpretation of the Magnetic map

From the total field magnetic anomaly map of the study area (Fig. 4.4 a), one can see the presence of prominent anomalous features. In comparison to the reference geomagnetic of the latitude of the study area which about 35000 nT, the Gemeto area presents both high and low amplitude anomalies.

Using the lesson obtained from the Bouguer gravity structure, representing the regional by a linear trend confirmed that the dominant features in the region follow a general NE – SW orientation. Removing these trends from the total map resulted in the residual anomaly map of the study area shown on figure 4.4 c.

On the residual magnetic anomaly map a uniquely darken area characterized by relatively the lowest magnetic values is observed. This anomalous region spatially coincides with area showing extremely low negative Bouguer gravity values. This was assumed to be one of the thermally affected areas where the rock units tend to have lower density and magnetic intensity as a result of thermal disorder. This in turn may mark the location possible heat source for the thermal springs in the area.

The other prominent feature observed from the residual map is that, the local magnetic highs and lows are separated by linear structures predominantly in the NE-SW direction. These linear structures are interpreted to represent near surface fractures/faults. Firsthand field observations further reinforce such speculations as there exist a number of thermal manifestations, including a natural thermal pool (cover photo), in these localities that may use the structures as conduits to and from the subsurface hydro-thermal chamber(s).

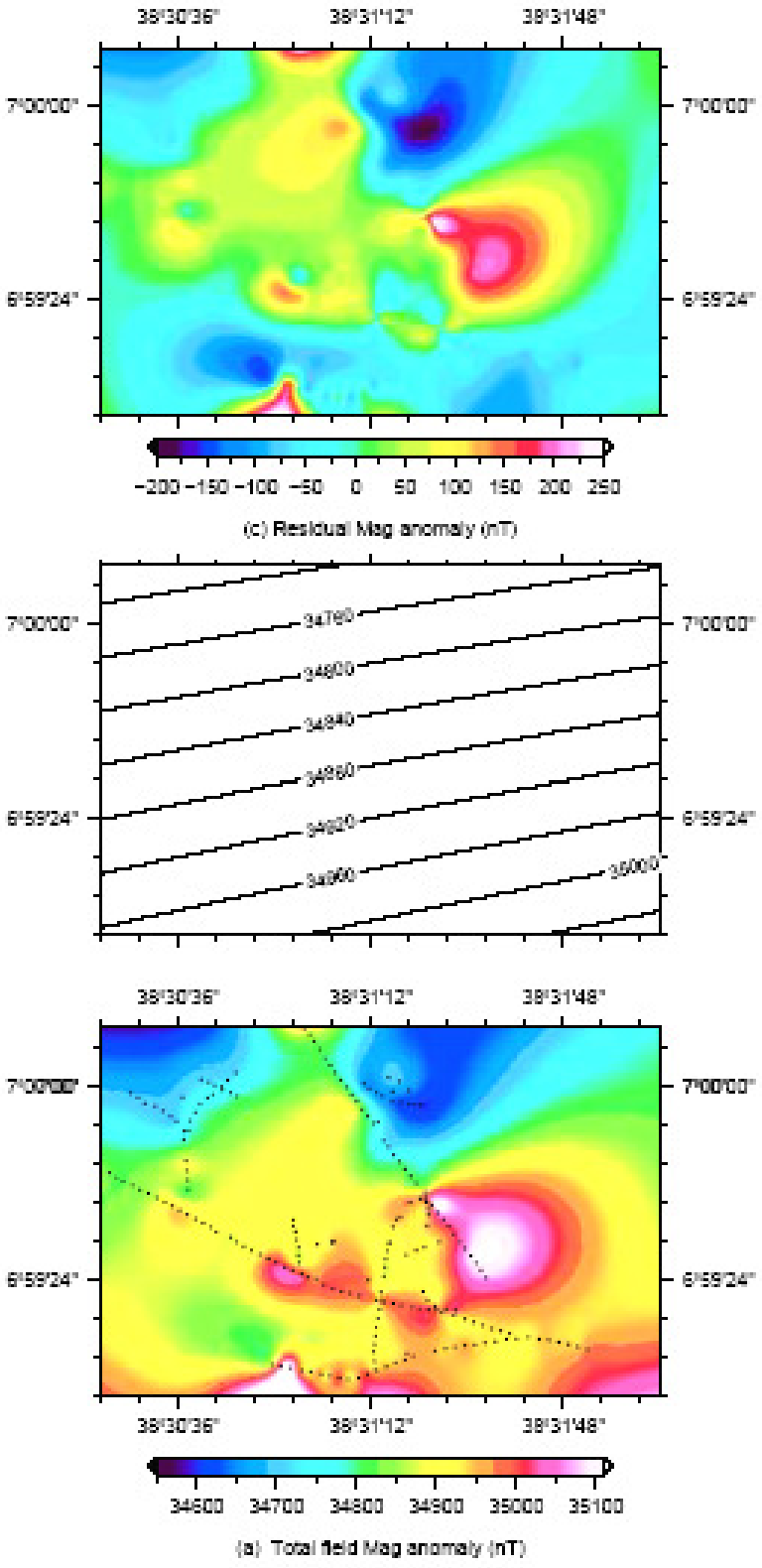

Fig.4.4 Magnetic anomaly maps of Gemeto area

The residual magnetic anomaly map also shows low magnetic anomaly region from the right bottom of the map indicating extension of the NE-SW shallow structure which may be one of the path that recharges the area from this side.

4.2.2.2 Quantitative Interpretation of the Magnetic profiles

The 2-D models along both profiles (Fig. 4.5 & 4.6) indicate that the magnetic susceptibility of the rock units in the area rapidly decreases down ward. On profile 1, the middle subsurface blocks exhibit the lowest susceptibility ranges as compared to the neighboring rock units and their lateral limits coincide to the probable locations of the linear structures discussed above. These regions seem to correspond to the hydro-thermally affected region discussed above. This may be due to the fact that magnetic susceptibility decreases with increasing temperature.

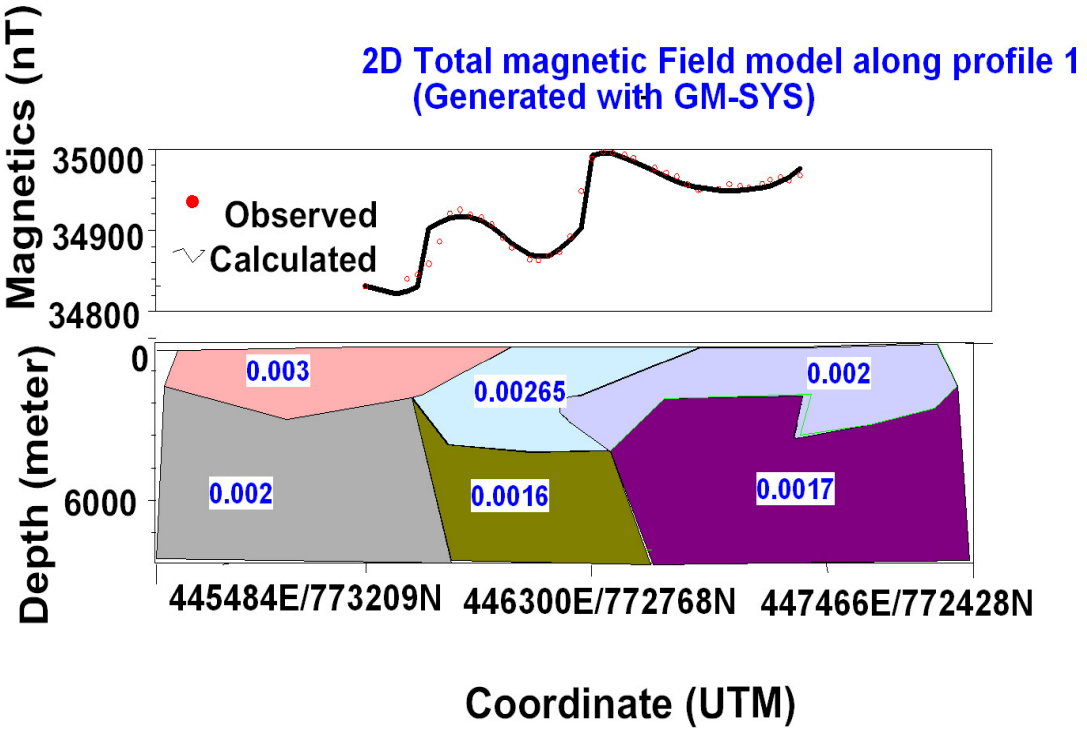

Fig.4.5 2-D Magnetic model of Gemeto area along profile 1

The 2-D model of profile two is also in a good agreement to the above results. Furthermore, the 2-D model of profile two indicates that the magnetic susceptibility response of the subsurface rocks gradually stabilizes and gets its minimum value at about 5km, probably indicating the depth at which the local thermal gradient flattens. This may indicate the possible depth of the heat source in the area. The maximum amplitude and short wave length of magnetic field around the middle blocks of profile 2 are indicators of shallow structure. It may be the NE-SW lying structure proposed from the magnetic anomaly map.

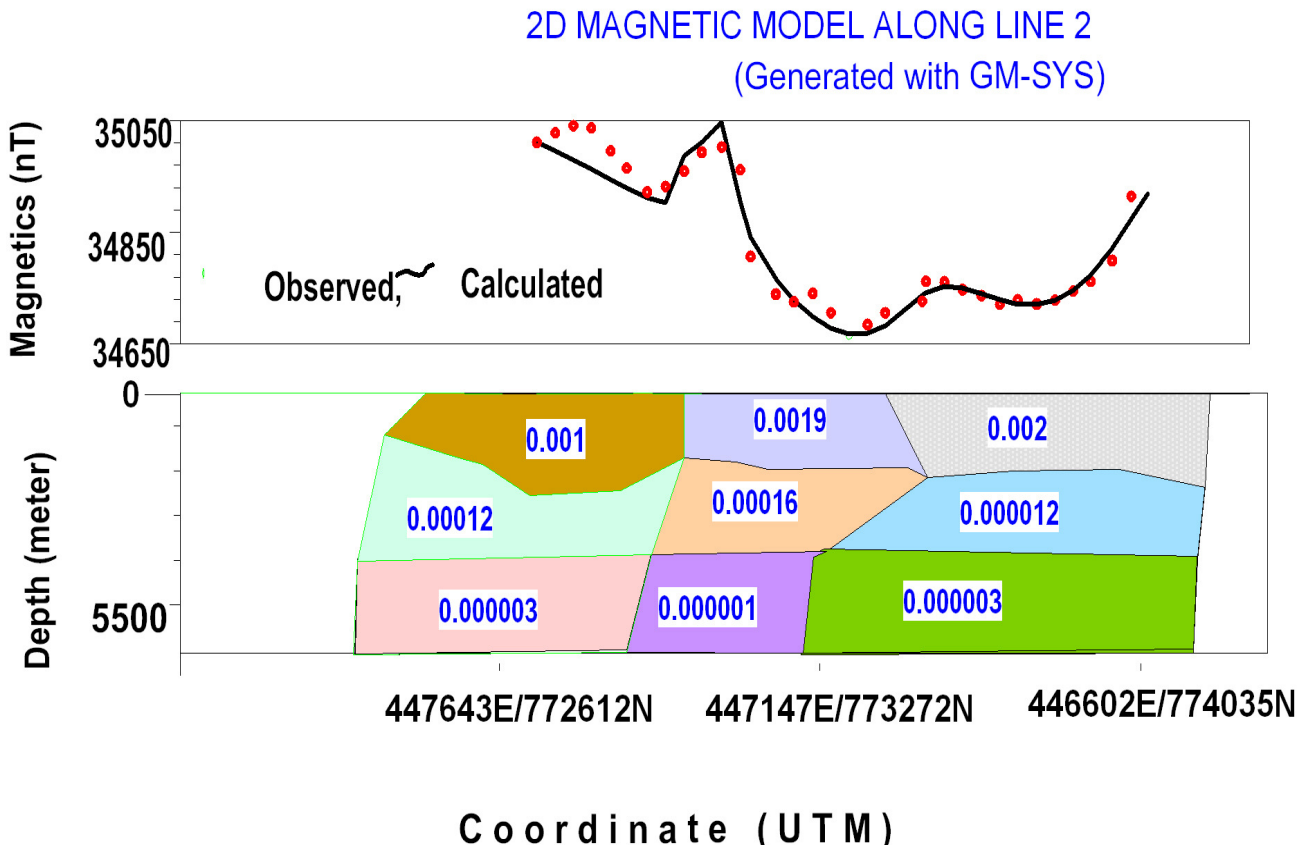

Fig.4.6 2-D Magnetic model of Gemeto area along profile 2

4.3 The Electrical Resistivity Method

4.3.1 Instrument and Data Acquisition

The equipment used for the survey included a PASI 16GL Earth Resistivity Meter, P300 Booster\Energizer with appropriate electrodes, cables on reels, and other accessories.

At each of the sounding points a maximum current electrode separation AB/2 was thought to be adequate to map the potential aquifer zones.
The survey is carried out along one profile which is approximately along one of the magnetic profile (P1). A total of four VES points has been taken using Schlumberger electrode array with the spacing between successive VES points of about 300m.

4.3.2 Data Processing and Interpretation

The object of geophysical interpretation of resistivity sounding data is to determine the thickness and resistivity of different horizons by studying the resulting field curves and use these results to obtain geological picture of the area under investigation.
The inversion program, RESIXIP, is used in this work for the determination of the final model parameters. The program undergoes a number of iterations as commanded by the user until the calculated error becomes the least error limit. By this process the resistivity and depth values the constituent layers are determined for each VES is determined.

4.3.2.1 Apparent resistivity Pseudo-section

Pseudo-section along the profile from the apparent resistivity values is constructed using mapping software “surfer 8” and qualitatively shows the lateral and vertical variations electrical properties with in the subsurface.
A conductive overburden of variable thickness occupies the top of the section and is underlain by relatively resistive substratum. The resistive bottom section lacks continuity and appears as dome like structure right beneath VES -2 plunging to either side of the survey line. However, the resistive bottom tends to reappear again on either flank and appears as separated from the central dome by some sort of geologic structure, likely a fault plane.

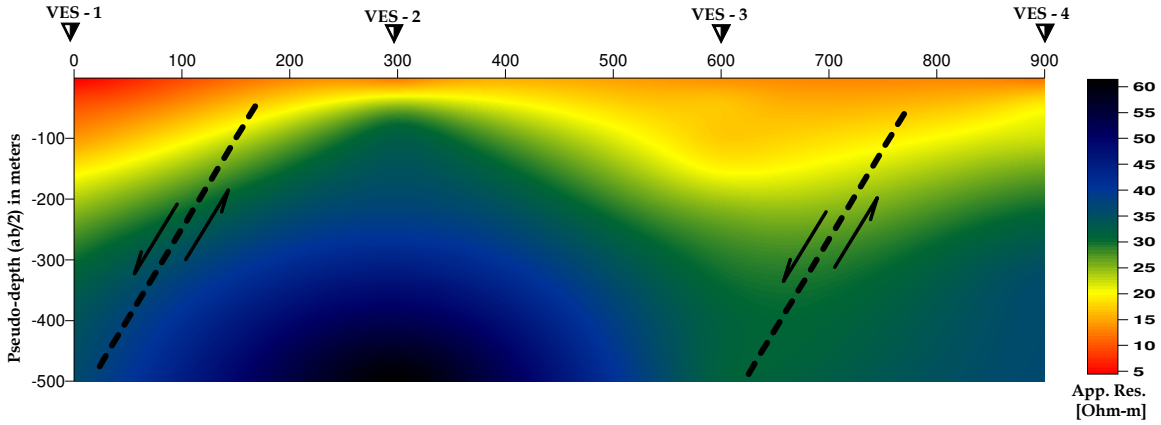

Fig. 4.7 Electrical resistivity pseudo-section

4.3.2.2 Geoelectric section

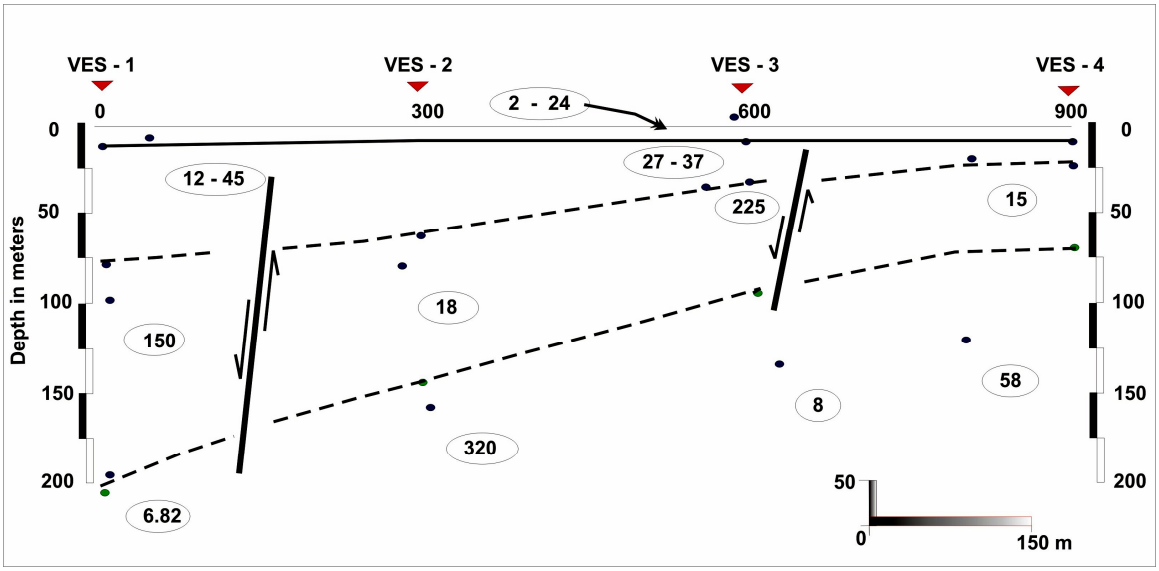

Fig. 4.8 Geoelectric section of the profile

The geoelectric sections have a four layered subsurface structure. The topmost layer is a uniformly thin layer whose thickness varies from 0.4m to 10.3m.

The resistivity of this top layer generally varies from 2 Ω m to 24 Ω m. Here the variation in resistivity values of top layer could result from the variation in moisture (water) content contained in the top soil of the wet marshy ground and relatively dry alluvial deposits.

A second layer of thickness 60m around VES1 and 20m around VES4, with resistivity varying between 12 Ω m to 37 Ω m is supposed to constitute of clay. Beginning from the third geoelectric layer the variation in layer thickness as well as apparent resistivity values are indicators of presence structural disturbance in the area.

In between VES1 and VES2 the apparent resistivity values as well as layer thickness increase rapidly. This feature is also observed on the Pseudosection map. In the vicinity of VES2 the apparent resistivity value achieves its maximum. This may be interpreted as rhyolitic lava which is common in the area. Between VES3 and VES4 depressed structure that inclined down from VES4 to VES3 is observed. This structure that inclined down from NE to SW direction is also detected on the magnetic anomaly map and interpreted as the shallow structure that recharges the area. Information from geoelectric section and pseudosection are thus in a good conformity with magnetic anomaly map response.

The fact that the study area is characterized by the lowest topography and affected by faults permit localized recharge.

CHAPTER FIVE

5. CONCLUSIONS AND RECOMMENDATIONS

5.1 CONCLUSIONS

The main conduits for the propagation of heat from the deep-seated thermal sources are thought to be the regional faults and fractures which also transect the Gemeto area. The result of the regional Bouguer gravity analysis clearly shows the general trends of these structures. The orientation of these regional structural trends was shown to be concordant to that of the eastern escarpment of the rift lying, approximately, NE - SW direction.

Results from local magnetic and electrical resistivity studies reveal anomalous signatures related to shallow, highly fractured/faulted structures in the area. Most of these shallow structures are oriented NNE-SSW and N-S direction. These shallow structures facilitate deep and shallow circulation of ground water in the area.

The heat source responsible for thermal springs manifested around Gemeto area may be cause by either shallow, young magmatic intrusions that are probably facilitated by cross faulting where the rhyolites are produced by differentiation or high regional heat flow in deep fault controlled meteoric water.

Results obtained in this work have so far revealed that though the abundant geologic structures may favor and facilitate large amount of water circulation, the signature of heat source in this area seems localize.

Even though detail geological hydrogeological and geophysical survey is important for its complete description, all the geophysical results described and discussed in the present study indicate that the Gemeto thermal springs has all the necessary geothermal potential for small scale projects such as resort development and thermal therapy centers.

5.2 RECOMMENDATIONS

Based on the main findings of this study, the following recommendations are given:

1. Inductive Electromagnetic methods such as large loop Transient Electromagnetics (TEM) and Magneto-Telluric (MT) have currently been used in geothermal projects for their potential to probe larger depth than galvanic counterpart (DC Resistivity). Enhanced capability in delineating subsurface horizons of anomalous heat and/or fluid concentration makes these methods indispensable tools in appraisal of geothermal resources and their subsequent utilization. It is, therefore, worth any effort to plan electromagnetic campaign for Gemeto thermal springs.

2. Although regional gravity data obtained from Ethiopian Geological Survey has revealed plenty of information, there is still data gap around the study area. Therefore, it is recommendable to collect additional gravity data at and around the study area and.

3. Implementations of the above recommended geophysical investigations should be supplemented by other studies from related fields. Integrating the geophysical results to hydrogeological, geo-structural and heat flow model is mandatory before qualifying the area for large-scale geothermal energy development.

REFERENCES

Abera, A., 1983. Crustal modeling from gravity data in the Ethiopian rift. M.Sc. thesis, Addis Ababa University, Addis Ababa, Ethiopia.

Abera, A., 1992. the gravity field and crustal structure of the main Ethiopian rift. Ph.D. thesis, royal institute of technology, Department of geodesy, report No.26 (TRITA GEOD1026), Stockholm Sweden.

Befekadu, O., 1989 The application of gravity and electrical resistivity survey to geothermal exploration in the main Ethiopian rift, M.Sc. thesis, University of Liecester.

Befekadu, O., Abiy,H., and Kesela (1983): Geophysical survey in the Aluto-Langano Geothermal Field.

Dessie, N., (1997). Hydrogeology of Awassa area, unpub. M.Sc. thesis, AAU, Addis Ababa, 106pp.

Dobrin, M.B.,and Savit,C.H., 1988. introduction to geophysical prospecting. MCGraw. Hill Inc. Singapore.

Duprat, A. (1987): Geophysics in geothermal prospecting. Applied Geothermic. John Wiley & Sons. Ltd.

Ebniger, C.J., Yemane, T., WoldeGabriel, G., Aronson, J.L., & Walter, R.C., 1993. Late Eocene-Recent volcanism and faulting in the southern main Ethiopian rift. J. Geol. Soc., London,150, 99-108

Edwin, S., Robinson, CAHIT CORUH, (1988). Basic Exploration Geophysics.

G. WoldeGabriel, R.C. Walter, W.K. Hart, S.A., Mertizman, J.L., Aronson, Temporal relations and geochemical features of the felsic volcanism in the central sector of the main Ethiopian Rift, Acta, Volcanologica, Vol. 11(1)-1999: 53-67

Gezahgn,Y.,1980. Geothermal study in the northwest lake, Abaya area. M.Sc. thesis. Addis Ababa university. Addis Ababa, Ethiopia.

Gianelli, G., & Teklemariam, M. 1993. water rock interaction processes in the Aluto Langano geothermal field (Ethiopia). Journal of volcanology and geothermal research, 56,429-445.

Gibson, I., L.,1969. structural and geology of an axial portion of the main Ethiopian rift . Tectonophysics 8: 561-568.

Gidey. WoldeGabriel, Aronson, J.L., and Walter, R.C., (1990). Geology, Geochronology and rift basin development in the central sector of the the MER, Geol. Sco. AM.Bul.,102,439-458.

Harbie, H., (2001), Geophysical Survey of the shalla caldera and its environs, for the exploration of geothermal energy. Unpub. M.Sc. thesis, Addis Ababa university, Addis Ababa, Ethiopia.

John, M. Reynolads, (1997) An introduction to applied and environemental Geophysics.

Jose, A.S., Pabblo, C.L., and Antonio, P.G.(2004). Evaluation of geothermal flow at the springs in Aragon, Spain, and its relation to geologic structures, Hydro. Jour., 12, 601-609

Kazmin, V.,1979. Stratigraphy and correlation of volcanic rocks in Ethiopia. EIGS, note No. 106: 1-26

Kenneth. and Grant, H., (1992) Volcanology and Geothermal Energy, University of California Press.

Mohr, P.A.,1967c. Major volcano-Tectonic Lineament in the Ethiopian rif system: Nature, V.213, P.664-665.

Mohr, P.A., (1971). The geology of Ethiopia. Addis Ababa University Press, Addis Ababa, Ethiopia

Mortiz, H.,1971. Geodetic reference system 1967. Pub. No3, Bulletin Geodesique, Paris.

Parasnis,D.S., (1989): Principles of applied Geophysics. Chapman and Hall, London, England.

Searle. R.C., and Gouin, P.,1972. Gravity of the central part of the Ethiopian rift.

Tadesse, D., and Zenaw, T. (2003) Hydrogeology and engineering geology of Awassa lake catchments, unpub. Report,Geological Survey of Ethiopia, Addis Ababa.

Tamiru, A. and Vernier, A.,1997. Conceptual model for Boku hydrothermal area (Nazreth) Main Ethiopian Rift Valley. SINET. J.Sci. 20(2): 283-291, Addis Ababa University, Addis Ababa, Ethiopia.

Telford, W.M., Sheriff, R.E., and Geldart, L.P., 1990. Applied Geophysics. Second edition Cambrdge.

Tenalem, A., (1998) the hydrogeological system of the Lake District basin, Ethiopia unpub. Ph. D. thesis.

Tesfaye, C., 1982. Hydrogeology of lakes region. Ministry of Mines and Energy, Ethiopian Institute of Geological Survey, Memoir No.7, P97, Addis Ababa, Ethiopia.

Tibebu, A., (2001), Geophysical Studies in the Aluto Geothermal area, unpub. M.Sc. thesis, Addis Ababa University, Addis Ababa, Ethiopia.

Tigistu, H., Tamiru, A., and Shimeles, F., Integrated Geophysical investigations to study thermal zones at Boku Volcanic center, Main Ethiopian Rift. SINET: Ethiopian, J. Sci., 25(2) 253-262, 2002.

UNDP, (1973). Investigation of geothermal resources for power development: Geology, Geochemistry and hydrogeology of hot springs of east Africa rift system with in Ethiopia. (Tech. Rpt. DP/SF/UN/116 No.275) UNDP, New York.

Wondwosen, M., (2005) Conceptualization of ground water flow system and aquifer characterization in Awassa lake catchments, unpub. M.Sc. thesis, Addis Ababa University Addis Ababa, Ethiopia.

Zemenu, G. (2000), Engineering geology of Awassa area, unpub. M.Sc. thesis, Addis Ababa University 132pp. Addis Ababa, Ethiopia.